

On Dessins d'Enfants to Seiberg-Witten Curves and Conformal Blocks

Jiakang Bao,^a Omar Foda,^b Yang-Hui He,^{a,c,d} Edward Hirst,^a James Read,^e Yan Xiao,^f Futoshi Yagi^g

^a*Department of Mathematics, City, University of London, EC1V 0HB, UK*

^b*School of Mathematics and Statistics, University of Melbourne, Royal Parade, Parkville, VIC 3010, Australia*

^c*Merton College, University of Oxford, OX1 4JD, UK*

^d*School of Physics, NanKai University, Tianjin, 300071, P.R. China*

^e*Pembroke College, University of Oxford, OX1 1DW, UK*

^f*Department of Physics, Tsinghua University, Beijing, 100084, China*

^g*School of Mathematics, Southwest Jiaotong University, West Zone, High-Tech District, Chengdu, Sichuan, 611756, China*

E-mail: jiakang.bao@city.ac.uk, omar.foda@unimelb.edu.au,
hey@maths.ox.ac.uk, edward.hirst@city.ac.uk, jimeree@gmail.com,
steven1025xiao@gmail.com, futoshi.yagi@swjtu.edu.cn

ABSTRACT: We consider the complete set of six trivalent Grothendieck dessins d'enfants with 4 punctures on the sphere, interpret their algebraic curves as Seiberg-Witten curves, then use the mirror map and the AGT map to obtain the corresponding 4d $\mathcal{N} = 2$ supersymmetric instanton partition functions and 2d Virasoro conformal blocks. We find that the parametrizations obtained from a dessin should be related by certain duality as gauge theories. As the parametrizations are discrete, it is also natural to conjecture that they correspond to the spectra of minimal models. In particular, the parametrizations become continuous when $c = 1$, just like the spectra of minimal models in the limit $c \rightarrow 1$.

Contents

1	Introduction	1
2	From Conformal Blocks to Dessins d’Enfants	3
2.1	From 2d Conformal Blocks to 4d Instanton Partition Functions	3
2.2	From 4d to 5d Instanton Partition Functions and A-Model Topological String Partition Functions	8
2.3	From Topological String Partition Functions to Seiberg-Witten Curves	10
2.4	From Seiberg-Witten Curves to Dessins d’Enfants	14
3	From Dessins to Conformal Blocks	17
3.1	The SU(2) with 4 Flavours	17
3.2	Example: $\Gamma(3)$	20
3.3	Matching Parameters	25
4	Conclusions and Outlook	33
A	The B-model and Omega Deformations	34
B	Brane Configurations	35
B.1	The Type IIA Brane Configuration	35
B.2	The M-theory Brane Configuration	36
C	Congruence Subgroups of the Modular Group	37
D	Elliptic Curves and j-Invariants	38
	References	39

1 Introduction

Consider a 4-point conformal block (CB) in a 2d conformal field theory (CFT) based on $\mathcal{W}_2 \times \mathcal{H}$, where \mathcal{W}_2 is the Virasoro algebra and \mathcal{H} is the Heisenberg algebra. Using the Alday-Gaiotto-Tachikawa (AGT) correspondence [1], this is identified with an instanton partition function in an $\mathcal{N} = 2$ supersymmetric Yang-Mills (SYM) theory, with an SU(2) gauge group and four fundamental hypers.

The low energy physics of this gauge theory is described in terms of a Seiberg-Witten (SW) curve and the SW differential on it [2, 3]. Then in [4], a method of instanton counting was introduced to find these low energy solutions to SW theories. Later, the S-duality for $\mathcal{N} = 2$ supersymmetric systems was studied in [5]. In recent works [6–12], connections between Grothendieck’s dessins d’enfants on the one hand and 4d $\mathcal{N} = 2$ SYM on the other were studied. In this note, we further explore these connections and extend them to 2d conformal field theory. We focus on the set of six trivalent dessins with 4 punctures on the sphere, which, as we will see, are related to a simple and important class of 4d $\mathcal{N} = 2$ SYM theories and conformal blocks in 2d conformal field theory.

From these dessins, we obtain algebraic curves that we interpret as SW curves of 4d $SU(2)$ $\mathcal{N} = 2$ $N_f = 4$, SYM theories. These curves are given in terms of six parameters, four mass parameters $(\mu_1, \mu_2, \mu_3, \mu_4)$, a parameter ζ and a modulus U . We write these curves in the form that appears in [13], and use their mirror map to translate the above six parameters to the six parameters that characterize the 4d instanton partition function of a 4d $\mathcal{N} = 2$ SYM theory. In particular, we map the modulus U to the Coulomb parameter a . Following that, we use the AGT dictionary to interpret the result in 2d CFT terms.

Let us take a closer look at the six parameters for the $SU(2)$ gauge theory. With $N_f = 4$, the theory has an $SO(8) = SU(2)^4$ flavour symmetry. Then μ_i ’s denote the mass parameters for the four fundamental hypers. These parameters would be identified as the momenta of the primaries in Liouville theory under AGT correspondence. As usual, we would arrange the poles of the SW curves at $z = 0, 1, \infty$ and ζ . This ζ is nothing but the UV gauge coupling τ via $\zeta = \exp(2\pi i\tau)$. For each dessin, we find that ζ could have several different values but these values enjoy certain triality.

Recall that the the Coulomb parameter a denotes the vev of the adjoint scalar ϕ , or equivalently, a could be obtained by integrating the SW differential along the so-called A -cycle on SW curve. Such supersymmetric vacua can be gauge invariantly parametrized by $u = \langle \text{tr}\phi^2 \rangle / 2 = a^2$ up to quantum corrections (and hence the name u -plane). Following [14], the parameter U , which will appear in the parametrization of the curve, is linear in the Coulomb moduli u . In fact, as we will see, each dessin gives a family of solutions for a ’s and U ’s, and indeed, we would have the same corresponding dessin under the change $a \rightarrow ka, U \rightarrow k^2U$ for some real k . This is consistent with our relation $a^2 \sim u \sim U$.

The paper is outlined as follows. In §2, we start from the CFT side and review the AGT correspondence to get the corresponding partition functions. Then from A-model topological strings, we obtain the SW curve for $SU(2)$ with 4 flavours and thence the dessins. In §3, we reverse the discussion and six particular dessins would yield

specific parametrizations for SW curves, which following our dictionary immediately provides the parametrizations for the conformal blocks. In the appendices, we give some background on brane systems as well as elliptic curves.

2 From Conformal Blocks to Dessins d’Enfants

Before we derive the results in 2d CFT from the 6 dessins with 4 punctures on the sphere, we give a brief review of different subjects including CBs, partition functions, SW curves and dessins, following a route map from CBs to dessins.

2.1 From 2d Conformal Blocks to 4d Instanton Partition Functions

It is conjectured that there is a connection between 2d Liouville CFTs and $SU(2)$ supersymmetric gauge theories in 4d with $\mathcal{N} = 2$. The free parameters of the two areas are naturally mapped to each other under AGT correspondence. We first start with the CFT side.

Conformal Blocks Conformal blocks form a basis of the vertex operator (VO) algebra, used when performing a particular operator product expansion (OPE) of a correlation function. They are a key ingredient in the conformal bootstrap approach to calculating these correlators in 2d CFTs. Global conformal Ward identities of the CFT allow 2-point functions to be completely determined, whilst 3-point functions to have fixed results up to their respective structure constants. Thus when calculating an $N \geq 4$ -point function the recursion of applying OPEs allows expression of the correlator in terms of these simpler 3-point function structure constants, and conformal blocks.

More specifically, an OPE amounts to summation over all representations of the vertex operator algebra. In the common case where this algebra factorises into two Virasoro algebras the sum includes all combinations of the left and right Virasoro algebras’ representations for the CFT. Each term in the sum has a product of two conformal blocks, one in each of the term’s left and right representations respectively.

Conformal blocks in general are sums over the states in their representation, they’re functions of the fields’ positions & conformal dimensions, the conformal dimension of the basis expansion, and the central charge of the algebra. Blocks over primary fields have simpler properties, whilst those including descendent fields can be determined with use of local Ward identities. If the correlator in question includes a degenerate field then BPZ equations need to be enforced, which can simplify conformal block computations [15].

In the classic example of 4-point functions, the Global Ward identities allow Möbius transformation, mapping 3 of the 4 complex coordinates to $\{0, \zeta, 1, \infty\}$, leaving a single ‘cross-ratio’ coordinate ζ for the conformal blocks to be a function of. Explicitly

$$\left\langle \prod_{i=1}^4 V_i(\zeta, \bar{\zeta}) \right\rangle = \sum_{R, \bar{R}} C_{12R} C_{34\bar{R}} \mathcal{F}_R(\{\Delta_i\}, \zeta) \mathcal{F}_{\bar{R}}(\{\bar{\Delta}_i\}, \bar{\zeta}) \quad (2.1)$$

for Virasoro operators V_i , of conformal dimension $(\Delta_i, \bar{\Delta}_i)$, as functions of holomorphic and anti-holomorphic coordinates $(\zeta, \bar{\zeta})$ respectively. The sum is over the fields’ representations in the left and right Virasoro algebras, denoted R, \bar{R} ; with the sum including structure constants, C_{ijk} , and conformal blocks, \mathcal{F} . These highest-weight representations of the Virasoro algebra are described in terms of Verma modules. They are generated by primary states and are irreducible in the absence of degenerate fields (which are both primary and descendent due to their null vector).

Since fields in a correlator can be permuted without change to the result, this translates into allowing different OPEs of the same correlator as different conformal block bases are used for expansion. The equivalence of these OPEs leads to ‘crossing symmetry’ and introduces additional consistency constraints which allow structure constants and block dimensions to be calculated. This is the conformal bootstrap methodology, and leaves calculation of conformal blocks as the final ingredient for computing correlators [16].

Conformal blocks are traditionally computed via Zamolodchikov recursion methods, however in the cases of degenerate fields in the correlators the BPZ equations provide a shortcut to finding them. In special cases these blocks can be expressed simply - for example a 4-point function on the sphere with one degenerate field (with a 2nd order null vector) can be expressed in terms of hypergeometric functions.

The AGT correspondence then makes a connection between the conformal dimensions of the fields in the correlator, and the coordinate ζ , with parameters arising in Nekrasov instanton partition functions, as subsequently described. With the help of this correspondence we then compute the conformal blocks associated to the 6 dessin considered in this study.

The Nekrasov Partition Function If we choose some dynamical energy scale Λ , for generic vev a , the general $\mathcal{N} = 2$ low energy effective action reads

$$\mathcal{L}_{\text{eff}} = \frac{1}{4\pi} \int d^2\theta d^2\tilde{\theta} \mathcal{F}(\Psi)(+c.c.), \quad (2.2)$$

where Ψ is the $\mathcal{N} = 2$ V-plet, and the holomorphic function \mathcal{F} is known as the *prepotential*. Then we can write the path integral

$$\int [DX] e^{i \int d^4x \mathcal{L}_{\text{eff}}} \quad (2.3)$$

for the light fields X in the V-plet. First conjectured in [4] and then proven in [17], the prepotential can be solved by

$$\mathcal{F} = \lim_{\epsilon_{1,2} \rightarrow 0} \epsilon_1 \epsilon_2 \log Z_{\text{Nek}}, \quad (2.4)$$

where ϵ_i 's are known as the deformation parameters, and Z_{Nek} is the *Nekrasov partition function*. The Nekrasov partition function has two factors:

$$Z_{\text{Nek}} = Z_{\text{pert}} Z_{\text{inst}}, \quad (2.5)$$

where Z_{pert} is the perturbative partition function and Z_{inst} denotes the contribution from instantons. Due to non-renormalization theorem, Z_{pert} only has tree level and 1-loop level factors: $Z_{\text{pert}} = Z_{\text{cl}} Z_{1\text{-loop}}$. Then

$$\lim_{\epsilon_{1,2} \rightarrow 0} \epsilon_1 \epsilon_2 \log(Z_{\text{cl}} Z_{1\text{-loop}} Z_{\text{inst}}) = \mathcal{F}_{\text{cl}} + \mathcal{F}_{1\text{-loop}} + \mathcal{F}_{\text{inst}}. \quad (2.6)$$

We will now focus on the instanton partition function Z_{inst} . For $\text{SU}(2)$ quiver theories, the Coulomb branches are parametrized by the Coulomb moduli $\vec{a} = (a_1, a_2) = (a, -a)$. Each Coulomb modulus is associated with a Young tableau Y , in which every box is labelled by a pair $s = (i, j)$ to denote its position. Hence, the instanton partition function depends on $\vec{Y} = (Y_1, Y_2)$, the vev a , and possibly the mass m of matter in the theory. Let us define [13]

$$E(a, Y_1, Y_2, s) := a - \epsilon_1 L_{Y_2}(s) + \epsilon_2 (A_{Y_1}(s) + 1) \quad (2.7)$$

with

$$L_{Y_2}(s) = k_i - j, \quad A_{Y_1}(s) = k'_j - i, \quad (2.8)$$

where k_i is the length of i^{th} row of Y_2 , and k'_j is the height of j^{th} column of Y_2 . Let I, J label the gauge nodes. Then

$$\begin{aligned} & z_{\text{bifund}}(a^I, \vec{Y}^I; a^J, \vec{Y}^J; m) \\ &= \prod_{i,j=1}^2 \left(\prod_{s \in Y_i^I} (E(a_i^I - a_j^J, Y_i^I, Y_j^J, s) - m) \prod_{s \in Y_j^J} (\epsilon - E(a_j^J - a_i^I, Y_j^J, Y_i^I, s) - m) \right), \end{aligned} \quad (2.9)$$

where $\epsilon = \epsilon_1 + \epsilon_2$. For (anti-)fundamentals,

$$z_{\text{fund}}(\vec{a}, \vec{Y}, m) = \prod_{i=1}^2 \prod_{s \in Y_i} (\phi(a_i, s) - m + \epsilon), \quad z_{\text{antifund}}(\vec{a}, \vec{Y}, m) = z_{\text{fund}}(\vec{a}, \vec{Y}, \epsilon - m), \quad (2.10)$$

where $\phi(a_i, s) = a_i + \epsilon_1(i-1) + \epsilon_2(j-1)$. When we take one gauge group coupled to a bifundamental to zero (or weak) coupling, one may check from above that

$$\begin{aligned} z_{\text{bifund}}(\vec{a}, \vec{Y}^I; \vec{a}', \emptyset; m) &= z_{\text{fund}}(\vec{a}, \vec{Y}, m + a') z_{\text{fund}}(\vec{a}, \vec{Y}, m - a'); \\ z_{\text{bifund}}(\vec{a}', \emptyset; \vec{a}, \vec{Y}^I; m) &= z_{\text{antifund}}(\vec{a}, \vec{Y}, m + a') z_{\text{antifund}}(\vec{a}, \vec{Y}, m - a'). \end{aligned} \quad (2.11)$$

For adjoint chiral and vector multiplets,

$$z_{\text{adj}}(\vec{a}, \vec{Y}, m) = z_{\text{bifund}}(\vec{a}, \vec{Y}; \vec{a}, \vec{Y}; m), \quad z_{\text{vec}}(\vec{a}, \vec{Y}) = \frac{1}{z_{\text{adj}}(\vec{a}, \vec{Y}, 0)}. \quad (2.12)$$

The AGT correspondence First introduced in [18], Liouville theory has the Lagrangian description:

$$S = \frac{1}{4\pi} \int d^2\xi \sqrt{g} (g^{ad} \partial_a \phi \partial_d \phi + QR\phi + 4\pi\mu e^{2b\phi}), \quad (2.13)$$

where the first term is just the kinetic term of the free scalar ϕ . The second term is the curvature coupling with coupling constant Q and Ricci scalar R . The third term is the Liouville potential. Since the key elements we will discuss below is independent of the value of the scalar [19], we can always choose a state with $\phi \ll 0$ such that the exponential potential is suppressed. Hence, let us first ignore this last term.

Under the conformal transformation

$$\phi(z', \bar{z}') = \phi(z, \bar{z}) - \frac{Q}{2} \log \left| \frac{\partial z'}{\partial z} \right|^2, \quad (2.14)$$

we find that classically the primary fields are of form $V_\alpha \equiv e^{2\alpha\phi}$, which transform as

$$e^{2\alpha\phi(z', \bar{z}')} = \left(\frac{\partial z'}{\partial z} \right)^{-\alpha Q} \left(\frac{\partial \bar{z}'}{\partial \bar{z}} \right)^{-\alpha Q} e^{2\alpha\phi(z, \bar{z})}. \quad (2.15)$$

Thus, the conformal dimensions are $(\Delta, \bar{\Delta}) = (\alpha Q, \alpha Q)$. Quantum mechanically, we can write the VO $V_\alpha =: e^{2\alpha\phi} :$ (where $: \dots :$ denotes the normal ordering as usual). Computing the OPE between the stress tensor¹ $T(z)$ and the VO yields

$$T(z)V_\alpha(z') = \frac{-\alpha(\alpha - Q)}{(z - z')^2} V_\alpha(z') + \dots \quad (2.16)$$

¹The stress tensor can be calculated by the usual steps of varying the action with respect to the metric, which gives $T_{zz} = T(z) = -(\partial\phi)^2 + Q\partial^2\phi$ and a similar expression for $T_{\bar{z}\bar{z}} = \bar{T}(\bar{z})$, with $T_{z\bar{z}}$ vanishing.

Therefore the quantum conformal dimension reads $\Delta = \alpha(Q - \alpha)$. Likewise, we can calculate the OPE:

$$T(z)T(z') = \frac{(1 + 6Q^2)/2}{(z - z')^4} + \dots \quad (2.17)$$

Hence, the central charge is $c = 1 + 6Q^2$.

Under translation $\phi \mapsto \phi + \delta$, the correlation function $\langle e^{2\alpha_1\phi} \dots e^{2\alpha_n\phi} \rangle$ will collect an extra phase $\exp\left(\sum_i \alpha_i \delta\right)$. For an invariant action, we would want $\sum_i \alpha_i = 0$. On the other hand, the variation of curvature coupling term yields an extra $2Q\delta$ term. To compensate this, we modify the momentum conservation condition to $\sum_i \alpha_i = Q$.

If we turn on the Liouville potential, then the exponential needs to be a marginal deformation to keep the theory being conformal [20]. This means that it should have conformal dimensions $(\Delta, \bar{\Delta}) = (1, 1)$. As a result, we need $b(Q - b) = 1$, or equivalently, $Q = b + 1/b$.

Now we are ready to bridge the CBs and instanton partition functions [1]. We can fix the scale by setting $\epsilon_1 = b, \epsilon_2 = 1/b$, such that $Q = \epsilon_1 + \epsilon_2 = \epsilon$. Consider a quiver consisting of an $SU(2)$ gauge group with 2 $SU(2)$ antifundamentals and 2 $SU(2)$ fundamentals with mass parameters $\mu_{1,2}$ and $\mu_{3,4}$ respectively. Then the instanton partition function reads

$$Z_{\text{inst}} = \sum_{Y_{1,2}} \frac{e^{2\pi i\tau(|Y_1|+|Y_2|)}}{(1 - e^{2\pi i\tau})^{\frac{1}{2}(\mu_1+\mu_2)(2\epsilon-(\mu_3+\mu_4))}} z_{\text{vec}}(\vec{a}, \vec{Y}) z_{\text{matter}}, \quad (2.18)$$

where the denominator corresponds to the decoupling of a $U(1)$ factor, and

$$z_{\text{matter}} = z_{\text{antifund}}(\vec{a}, \vec{Y}, \mu_1) z_{\text{antifund}}(\vec{a}, \vec{Y}, \mu_2) z_{\text{fund}}(\vec{a}, \vec{Y}, \mu_3) z_{\text{fund}}(\vec{a}, \vec{Y}, \mu_4). \quad (2.19)$$

The instanton number $|Y_i|$ is the number of boxes in Y_i . Then under the following AGT dictionary²,

$$\begin{aligned} \mu_1 &= \alpha_1 + \alpha_2 - \frac{Q}{2}, \quad \mu_2 = \alpha_1 - \alpha_2 + \frac{Q}{2}, \quad \mu_3 = \alpha_3 + \alpha_4 - \frac{Q}{2}, \quad \mu_4 = \alpha_3 - \alpha_4 + \frac{Q}{2}, \\ a &= \alpha_{\text{int}} - \frac{Q}{2}, \quad e^{2\pi i\tau} = \zeta, \end{aligned} \quad (2.20)$$

²Strictly speaking, we have abused the notation here for simplicity. First, the left hand sides, which will be obtained from the SW theory, have mass dimension 1 while the right hand sides are dimensionless. Therefore, to make them match, there is an implicit factor $\frac{1}{\sqrt{\epsilon_1\epsilon_2}}$ on the left, where $\epsilon_{1,2}$ also have mass dimension 1. Similarly, for b and Q , we should have $Q = b + 1/b = \epsilon_1/\sqrt{\epsilon_1\epsilon_2} + \epsilon_2/\sqrt{\epsilon_1\epsilon_2}$. Moreover, this dictionary is built upon the usual $\epsilon_{1,2} \rightarrow 0$ limit. However, to incorporate the finite deformation parameters as discussed in Appendix A, there should be a shift of the mass parameters obtained from the Nekrasov expansion. We will recover these two modifications in §3.

the instanton partition function is equal to $\mathcal{B}_{\alpha_{\text{int}}}(\alpha_i|\zeta)$, where the conformal block from $\langle V_{\alpha_1} V_{\alpha_2} V_{\alpha_3} V_{\alpha_4} \rangle$ as in (2.1) can be written as $\mathcal{F} = \zeta^{\Delta_{\alpha_{\text{int}}} - \Delta_{\alpha_1} - \Delta_{\alpha_2}} \mathcal{B}_{\alpha_{\text{int}}}(\alpha_i|\zeta)$ and ‘‘int’’ stands for (the primary in) the internal channel. One may check this perturbatively, and at level $|Y|_{\text{max}}$, $\mathcal{B}_{\alpha_{\text{int}}}$ and Z_{inst} should agree up to $\mathcal{O}(\zeta^{|Y|_{\text{max}}+1})$ [1, 21]. Notice that when we have $c = 1$ CBs, viz, $Q = 0$, the AGT relation is simplified to

$$\mu_1 = \alpha_1 + \alpha_2, \mu_2 = \alpha_1 - \alpha_2, \mu_3 = \alpha_3 + \alpha_4, \mu_4 = \alpha_3 - \alpha_4, a = \alpha_{\text{int}}, e^{2\pi i \tau} = \zeta. \quad (2.21)$$

2.2 From 4d to 5d Instanton Partition Functions and A-Model Topological String Partition Functions

For type II string/M-theory (whose brane configurations are discussed in Appendix B) compactified on a Calabi-Yau 3-fold, the amplitudes at genus g correspond to the A-model string amplitudes of the CY_3 which enumerates the holomorphic functions from genus g Riemann surfaces to the CY_3 [22, 23]. The topological amplitudes for toric CY threefolds can be computed by *topological vertices* introduced in [24]. A topological vertex is a trivalent vertex as the (black) dual graph of the (grey) toric diagram:



$$, \quad (2.22)$$

where Y_i 's are the Young tableaux associated to the legs, and $C_{Y_1 Y_2 Y_0}(q)$ is the factor associated to the vertex, which can be expressed in terms of Schur and skew-Schur functions [24]. Albeit not labelled explicitly, each leg also has a direction such that the three legs attached to the same vertex all have outgoing or incoming directions. Then each leg is assigned a vector $\mathbf{v}_i = (v_{i1}, v_{i2})$ in that direction, such that the sum of the three vectors vanishes due to charge conservation and $\det(\mathbf{v}_i, \mathbf{v}_{i+1}) = \pm 1$ ($i \in \mathbb{Z}_3$). Now two topological vertices



$$, \quad (2.23)$$

can be glued as

$$\sum_{Y_0} C_{Y_1 Y_2 Y_0}(q) (-1)^{(n+1)|Y_0|} q^{-n\kappa(Y_0)/2} Q_0^{|Y_0|} C_{Y_1' Y_2' Y_0^T}, \quad (2.24)$$

where κ is related to quadratic Casimir of the representation corresponding to $|Y_0|$, namely, $\kappa(Y_0) = \sum_i y_i(y_i - 2i + 1)$ with y_i being the number of boxes in the i^{th} row.

The framing number n equals $\det(\mathbf{v}_{\text{in}}, \mathbf{v}_{\text{out}})$, where the two vectors are chosen such that $\mathbf{v}_{\text{in}} \cdot \mathbf{v}_{\text{out}} > 0$. For instance, we can choose either $\mathbf{v}_{\text{in}} = \mathbf{v}_1, \mathbf{v}_{\text{out}} = \mathbf{v}'_1$ or $\mathbf{v}_{\text{in}} = \mathbf{v}_2, \mathbf{v}_{\text{out}} = \mathbf{v}'_2$. The parameter Q_0 is the (exponentiated) Kähler parameter for the 2-cycle corresponding to the line in the dual toric diagram.

In [25], the above is extended to *refined topological vertex* as

$$C_{Y_1 Y_2 Y_0}(\mathbf{q}, t) = \left(\frac{\mathbf{q}}{t}\right)^{(\|Y_2\|^2 + \|Y_0\|^2)/2} t^{\kappa(Y_2)/2} P_{Y_0^{\text{T}}} (t^{-\rho}; \mathbf{q}, t) \\ \times \sum_{\eta} \left(\frac{\mathbf{q}}{t}\right)^{(|\eta| + |Y_1| - |Y_2|)/2} s_{Y_1^{\text{T}}/\eta} (t^{-\rho} \mathbf{q}^{-Y_0}) s_{Y_2/\eta} (t^{Y_0^{\text{T}}} \mathbf{q}^{-\rho}), \quad (2.25)$$

where $P_{Y_0^{\text{T}}} (t^{-\rho}; \mathbf{q}, t)$ is the Macdonald function and $s_{\alpha/\beta}$'s are the skew-Schur functions. The squared double slash denotes the quadratic sum of the number of boxes in each row of the Young tableau. Notice that the three Young tableaux are not cyclically symmetric and Y_0 corresponds to the preferred leg for gluing. One may check that when the Ω -background parameters satisfy $\mathbf{q} = t$, we would recover the unrefined topological vertex.

Define the framing factors,

$$f_Y(\mathbf{q}, t) = (-1)^{|Y|} \mathbf{q}^{\|Y^{\text{T}}\|^2/2} t^{-\|Y\|^2/2}, \quad \tilde{f}_Y(\mathbf{q}, t) = (-1)^{|Y|} \mathbf{q}^{(\|Y^{\text{T}}\|^2 + |Y|)/2} t^{-(\|Y\|^2 + |Y|)/2}, \quad (2.26)$$

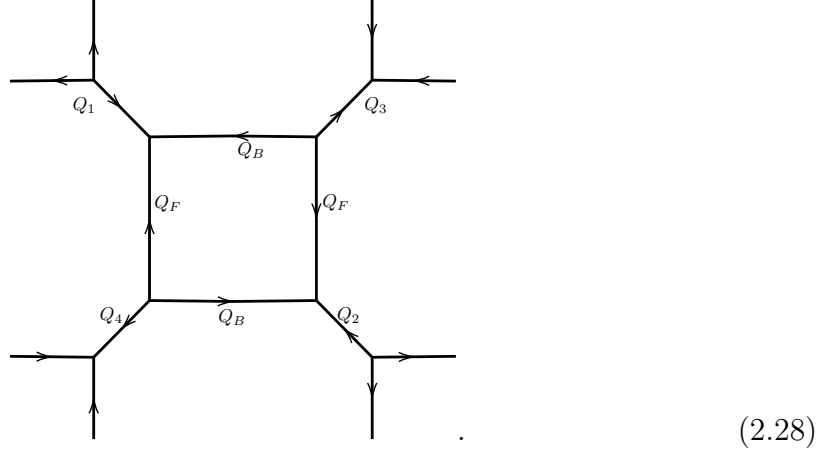
and the edge factor, $(-Q_0)^{|Y_0|} \times [\text{framing factor}]$. Then the topological string partition function takes the sum over all the Young tableaux of internal legs³ as [26]

$$Z_{\text{topo}} = \sum_{Y_i} \prod_{\text{edges}} [\text{edge factor}] \prod_{\text{vertices}} [\text{vertex factor}]. \quad (2.27)$$

Again, let us contemplate the $SU(2)$ gauge theory with 4 flavours. The dual toric

³The Young tableaux of external legs would be \emptyset .

diagram is



(2.28)

Following the gluing process, the partition function reads

$$\begin{aligned}
Z_{\text{topo}} &= \sum_{\lambda\rho\nu} (-Q_F)^{|\lambda_1|} \tilde{f}_{\lambda_1}(\mathbf{q}, t) (-Q_F)^{|\lambda_2|} \tilde{f}_{\lambda_2}(t, \mathbf{q}) (-Q_B)^{|\rho_1|} f_{\rho_1^T}(\mathbf{q}, t) (-Q_B)^{|\rho_2|} f_{\rho_2^T}(t, \mathbf{q}) \\
&\quad \times (-Q_1)^{|\nu_1|} (-Q_2)^{|\nu_2|} (-Q_3)^{|\nu_3|} (-Q_4)^{|\nu_4|} C_{\lambda_1^T \nu_3^T \rho_1^T}(\mathbf{q}, t) C_{\nu_4 \lambda_1 \rho_2}(\mathbf{q}, t) \\
&\quad \times C_{\lambda_2^T \nu_2^T \rho_2^T}(t, \mathbf{q}) C_{\nu_1 \lambda_2 \rho_1}(t, \mathbf{q}) C_{\nu_1^T \emptyset \emptyset}(\mathbf{q}, t) C_{\emptyset \nu_2 \emptyset}(\mathbf{q}, t) C_{\nu_4^T \emptyset \emptyset}(t, \mathbf{q}) C_{\emptyset \nu_3 \emptyset}(t, \mathbf{q}). \quad (2.29)
\end{aligned}$$

Recall the 4d instanton partition function (2.18), which can be lifted to 5d as [27]

$$\begin{aligned}
Z_{\text{inst},5\text{d}} &= \sum_{Y_{1,2}} \frac{R^{4(|Y_1|+|Y_2|)} e^{2\pi i \tau (|Y_1|+|Y_2|)}}{(1 - e^{2\pi i \tau})^{\frac{1}{2}(\mu_1+\mu_2)(2\epsilon - (\mu_3+\mu_4))}} z_{\text{vec}}(\vec{a}, \vec{Y}) z_{\text{matter}} \\
&= \sum_{Y_{1,2}} \frac{(R\Lambda)^{4(|Y_1|+|Y_2|)}}{(1 - e^{2\pi i \tau})^{\frac{1}{2}(\mu_1+\mu_2)(2\epsilon - (\mu_3+\mu_4))}} z_{\text{vec}}(\vec{a}, \vec{Y}) z_{\text{matter}}, \quad (2.30)
\end{aligned}$$

where R is the radius of the compactified dimension S^1 . It is discussed in [27–29] that under the parameter identification

$$\mathbf{q} = e^{-R\epsilon_1}, \quad t = e^{R\epsilon_2}, \quad Q_i = e^{-R(\mu_i - a)}, \quad Q_B = (R\Lambda)^4, \quad Q_F = e^{2Ra}, \quad (2.31)$$

we would get $Z_{\text{topo}} = Z_{\text{inst},5\text{d}}$. Notice that when $\epsilon_1 = -\epsilon_2$, i.e., $Q = \epsilon = \epsilon_1 + \epsilon_2 = 0$, we have the unrefinement $\mathbf{q} = t$.

2.3 From Topological String Partition Functions to Seiberg-Witten Curves

Given the SW curve Σ in hyperelliptic form, it is possible to translate into the form $\lambda^2 = q(z)$, where λ is the *Seiberg-Witten differential*, and $q(z)$ is the meromorphic quadratic differential on the Gaiotto curve \mathcal{C} . In this subsection, we demonstrate how

this translation runs for the theory with a single $SU(2)$ factor and $N_f = 4$. This theory will constitute our running example throughout the paper.

To begin, following §9.1 of [30], Σ for the $SU(2)$ with $N_f = 4$ theory in hyperelliptic form is

$$\frac{f}{\tilde{z}}(\tilde{x} - \tilde{\mu}_1)(\tilde{x} - \tilde{\mu}_2) + (f'\tilde{z})(\tilde{x} - \tilde{\mu}_3)(\tilde{x} - \tilde{\mu}_4) = \tilde{x}^2 - u, \quad (2.32)$$

where f and f' are complex numbers and u parametrizes the space of supersymmetric vacua, viz, the u -plane. The parameter $\tilde{\mu}_i$ is a mixing of the bare masses of hypers and the dynamical scale Λ . The tildes on the auxiliary variables x and z are due to the rescaling of them below. We first choose the coordinate of \tilde{z} so that $f' = 1$. Completing a square in \tilde{x} by defining

$$x = \tilde{x} + \frac{\frac{\zeta}{\tilde{z}}(\tilde{\mu}_1 + \tilde{\mu}_2) + \tilde{z}(\tilde{\mu}_3 + \tilde{\mu}_4)}{2(1 - \tilde{z} - \frac{\zeta}{\tilde{z}})}, \quad (2.33)$$

we obtain $x^2 = g(\tilde{z})$ where g has double poles at $c_{1,2}(f)$. Now rescale $z = \tilde{z}/c_1(f)$ so that the poles are at $z = 1, \zeta$, and we get

$$x^2 = \frac{P(z)}{z^2(z-1)^2(z-\zeta)^2} \quad (2.34)$$

for some quartic polynomial $P(z)$ determined by $\tilde{\mu}_i$, ζ and u .

Construction of SW Curves from Toric Diagrams For 5d gauge theories, the 5-brane web diagrams can be used to construct SW curves. In fact, such web diagram is exactly the same as the dual toric diagram in the geometric engineering in §2.2 [31, 32]. The standard algorithm of constructing SW curves from toric diagrams are studied in [33]. Here, we will still focus on $SU(2)$ with 4 flavours, where the web/dual diagram is reproduced in Figure 2.1, along with its toric diagram.

For each vertex (i, j) in the toric diagram, we assign a non-zero number c_{ij} . There are four boundaries, so the boundary conditions according to the toric diagram now are

$$\begin{aligned} |w| \gg 1, \quad c_{02}w^2 + c_{12}tw^2 + c_{22}t^2w^2 &= c_{22}w^2(t - t_1)(t - t_3), \\ |w^{-1}| \gg 1, \quad c_{20}t^2 + c_{10}t + c_{00} &= c_{20}(t - t_2)(t - t_4), \\ |t| \gg 1, \quad c_{20}t^2 + c_{21}t^2w + c_{22}t^2w^2 &= c_{22}t^2(w - \tilde{m}_1)(w - \tilde{m}_2), \\ |t^{-1}| \gg 1, \quad c_{02}w^2 + c_{01}w + c_{00} &= c_{02}(w - \tilde{m}_3)(w - \tilde{m}_4), \end{aligned} \quad (2.35)$$

where t and w can be thought of as the horizontal and vertical coordinates of the diagram respectively. For consistency, we further need the compatibility condition which reads

$$\tilde{m}_1 t_1^{-1} \tilde{m}_2 t_2 = \tilde{m}_3 t_3 \tilde{m}_4 t_4^{-1}. \quad (2.36)$$

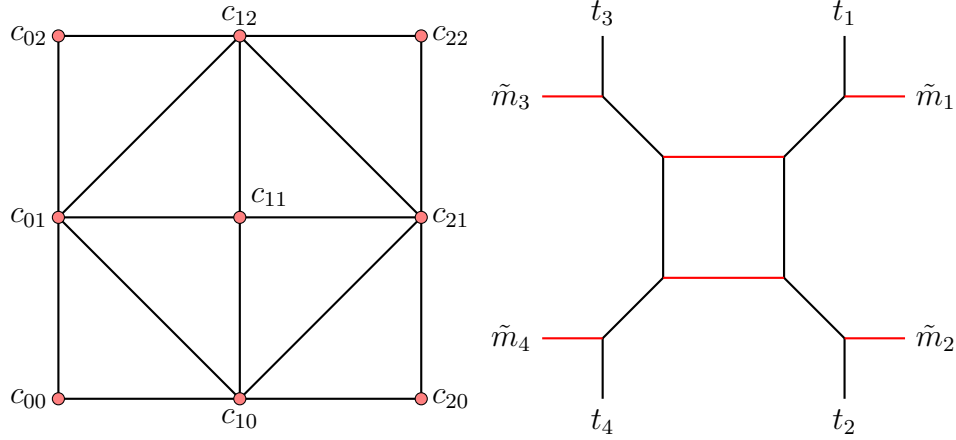


Figure 2.1: The toric diagram and its dual diagram for $SU(2)$ with 4 flavours.

Since SW curves are invariant under the rescaling of the coefficients, with the choice

$$c_{01} = c_{21} = 1, \quad c_{10} = c_{12} \quad (2.37)$$

we can determine all the coefficients living on the boundary, which leads to

$$\frac{t_1 + t_3}{t_2 + t_4} = \tilde{m}_1 \tilde{m}_2, \quad t_1 t_3 = \frac{\tilde{m}_1 + \tilde{m}_2}{\tilde{m}_3 + \tilde{m}_4}. \quad (2.38)$$

Hence, the curve is

$$\begin{aligned} 0 &= \sum_{i,j} c_{ij} t^i w^j \\ &= -\frac{1}{\tilde{m}_3 + \tilde{m}_4} (w - \tilde{m}_3)(w - \tilde{m}_4) + t \left(\frac{t_1}{\tilde{m}_1 + \tilde{m}_2} + \frac{1}{t_1(\tilde{m}_3 + \tilde{m}_4)} \right) (w^2 + Uw + 1) \\ &\quad - t^2 \frac{1}{\tilde{m}_1 + \tilde{m}_2} (w - \tilde{m}_1)(w - \tilde{m}_2), \end{aligned} \quad (2.39)$$

where $U = c_{11}$ is the only undetermined coefficient, which is interpreted as the Coulomb moduli parameter (see [33]). The gauge coupling is the geometric average of t_i , which is

$$q^{-1} \equiv \left(\frac{t_1 t_2}{t_3 t_4} \right)^{\frac{1}{2}}. \quad (2.40)$$

Defining a parameter $S \equiv \tilde{m}_1 \tilde{m}_2 \tilde{m}_3 \tilde{m}_4$, we have

$$t_1 = \left(\frac{\tilde{m}_1 + \tilde{m}_2}{\tilde{m}_3 + \tilde{m}_4} \right)^{\frac{1}{2}} \left(\frac{q^{-1} S^{\frac{1}{2}} - 1}{1 - q S^{\frac{1}{2}}} \right)^{\frac{1}{2}}. \quad (2.41)$$

Notice here the masses are all bare masses, which are related to the physical masses by

$$\tilde{m}'_i \equiv T \tilde{m}_i, \quad T = \left(\frac{q - S^{\frac{1}{2}}}{qS - S^{\frac{1}{2}}} \right)^{\frac{1}{2}}, \quad (2.42)$$

and a rescaling of t :

$$t \rightarrow t \sqrt{qS^{-\frac{1}{2}} T^2 \tilde{m}_1^2 \tilde{m}_2^2 \left(\frac{\tilde{m}_3 + \tilde{m}_4}{\tilde{m}_1 + \tilde{m}_2} \right)}. \quad (2.43)$$

We now have a compact form of t_1 ,

$$t_1 = \left(\frac{\tilde{m}_1 + \tilde{m}_2}{\tilde{m}_3 + \tilde{m}_4} \right)^{\frac{1}{2}} \left(\frac{q^{-1} S^{\frac{1}{2}} - 1}{1 - qS^{\frac{1}{2}}} \right)^{\frac{1}{2}} = \left(\frac{\tilde{m}'_1 + \tilde{m}'_2}{\tilde{m}'_3 + \tilde{m}'_4} \right)^{\frac{1}{2}} T q S^{-\frac{1}{2}}. \quad (2.44)$$

Defining a new $S' \equiv \tilde{m}'_1 \tilde{m}'_2 \tilde{m}'_3 \tilde{m}'_4$, the 5d $N_f = 4$ curve now is

$$\begin{aligned} & t^2 (w - \tilde{m}'_1) (w - \tilde{m}'_2) - t \left(w^2 \tilde{m}'_1 \tilde{m}'_2 \left(1 + q (S')^{-\frac{1}{2}} \right) + w U' + \tilde{m}'_1 \tilde{m}'_2 \left(1 + q (S')^{-\frac{1}{2}} \right) \right) \\ & + q (S')^{-\frac{1}{2}} (\tilde{m}'_1 \tilde{m}'_2)^2 (w - \tilde{m}'_3) (w - \tilde{m}'_4) = 0, \end{aligned} \quad (2.45)$$

where $U' = U \tilde{m}'_1 \tilde{m}'_2 \left(1 + q S'^{-\frac{1}{2}} \right)$.

The 4d limit curve Till now, the SW curve is a 5d curve, its 4d SW curve can be obtained by taking the vanishing limit of size of compactification circle $R \rightarrow 0$, where we have

$$w = e^{-Rv}, \quad \tilde{m}'_i = e^{-R\mu_i}. \quad (2.46)$$

In topological string theory, the 5d Coulomb parameter U' is an exponential

$$U' = e^{-Ru'}. \quad (2.47)$$

For the $N_f = 4$ curve, we then have the 4d limit

$$\begin{aligned} & t^2 (v - \mu_1) (v - \mu_2) + q (v - \mu_3) (v - \mu_4) + \\ & t \left(-(1+q)v^2 + v(\mu_1 + \mu_2) + \frac{1}{2}qv(\mu_1 + \mu_2 - \mu_3 - \mu_4) - vu' + (1+q)\mu_1\mu_2 \right) = 0. \end{aligned} \quad (2.48)$$

Redefining

$$u' = - \left(1 + \frac{1}{2}q \right) (\mu_1 + \mu_2) + \frac{3}{2}q(\mu_3 + \mu_4) + u \quad (2.49)$$

yields the curve

$$\begin{aligned} & t^2 (v - \mu_1) (v - \mu_2) + q (v - \mu_3) (v - \mu_4) \\ & + t \left(-(1+q)v^2 + qv \sum_{i=1}^4 \mu_i + (1+q)\mu_1\mu_2 - vu' \right) = 0. \end{aligned} \quad (2.50)$$

Reparametrization Let us rescale (2.50) as following

$$\mu_i \rightarrow \frac{\mu_i}{\sqrt{1+q}}, \quad v \rightarrow \frac{v}{\sqrt{1+q}}, \quad u' \rightarrow \frac{u'}{\sqrt{1+q}}, \quad (2.51)$$

so the curve now is

$$t(v - \mu_1)(v - \mu_2) - v^2 + \frac{qv \sum_{i=1}^4 \mu_i - vu'}{(1+q)} + \mu_1\mu_2 + \frac{q}{t}(v - \mu_3)(v - \mu_4) = 0. \quad (2.52)$$

Redefining

$$\begin{aligned} f/\tilde{z} = t, \quad f'\tilde{z} = q/t, \quad \tilde{x} &\equiv v + \frac{q \sum_{i=1}^4 \mu_i - u'}{2\sqrt{1+q}}, \quad \tilde{\mu}_i = \mu_i + \frac{q \sum_{i=1}^4 \mu_i - u'}{2\sqrt{1+q}}, \\ u &= \mu_1\mu_2 - \frac{q \sum_{i=1}^4 \mu_i - u'}{2\sqrt{1+q}}(\mu_1 + \mu_2) + \frac{1}{2} \frac{\left(q \sum_{i=1}^4 \mu_i - u' \right)^2}{1+q} \end{aligned} \quad (2.53)$$

recovers the curve of form (2.32), which is reproduced here:

$$\frac{f}{\tilde{z}}(\tilde{x} - \tilde{\mu}_1)(\tilde{x} - \tilde{\mu}_2) + (f'\tilde{z})(\tilde{x} - \tilde{\mu}_3)(\tilde{x} - \tilde{\mu}_4) = \tilde{x}^2 - u. \quad (2.54)$$

2.4 From Seiberg-Witten Curves to Dessins d'Enfants

We begin with a fresher on some preliminary definitions and key results [34, 35].

Definition 2.1. A dessin d'enfant, or child's drawing, is an ordered pair (X, \mathcal{D}) , where X is an oriented compact topological surface and $\mathcal{D} \subset X$ is a finite graph, such that

1. \mathcal{D} is a connected bipartite graph, and
2. $X \setminus \mathcal{D}$ is the union of finitely many topological discs that are the faces of \mathcal{D} .

There is a bijection between the dessins and Belyi maps known as the *Grothendieck correspondence* [36], where

Definition 2.2. A Belyi map β is a holomorphic map from the Riemann surface X to \mathbb{P}^1 ramified at only 3 points, which can be taken to be $\{0, 1, \infty\} \in \mathbb{P}^1$.

Recall that *ramification* means that the only points $\tilde{x} \in X$ where $\frac{d}{dx}\beta(x)|_{\tilde{x}} = 0$ are such that $\beta(\tilde{x}) = 0, 1$ or ∞ . In other words, the local Taylor expansion of $\beta(x)$ about the pre-images \tilde{x} of $\{0, 1, \infty\}$ have (at least) vanishing linear term.

From Belyi maps to dessins We can associate $\beta(x)$ to a dessin via its *ramification indices*: the order of vanishing of the Taylor series for $\beta(x)$ at \tilde{x} is the ramification index $r_{\beta(\tilde{x}) \in \{0,1,\infty\}}(i)$ at that i^{th} point. By convention, we mark one white node for the i^{th} pre-image of 0 with $r_0(i)$ edges emanating therefrom. Similarly, we mark one black node for the j^{th} pre-image of 1 with $r_1(j)$ edges. We then connect the nodes with the edges, joining only black with white, such that each face is a polygon with $2r_\infty(k)$ sides. In other words, there is one pre-image of ∞ corresponding to each polygon of \mathcal{D} . Moreover, there is a cyclic ordering arising from local monodromy winding around vertices, i.e., around local covering sheets that contain a common point.

The power of dessins comes from Belyi's remarkable theorem.

Theorem 2.1. *There exists an algebraic model of X (as a Riemann surface) defined over $\bar{\mathbb{Q}}$ iff there exists a Belyi map on X .*

Thus, the existence of a dessin on X is equivalent to X admitting an algebraic equation over the algebraic numbers. Moreover, the Galois group $\text{Gal}(\bar{\mathbb{Q}} : \mathbb{Q})$ acts faithfully on the space of dessins.

Quadratic Differentials A (holomorphic) quadratic differential q on a Riemann surface X is a holomorphic section of the symmetric square of the cotangent bundle. In terms of local coordinates z , $q = f(z)dz \otimes dz$, for some holomorphic function $f(z)$.

A curve $\gamma(t) \subset X$ can be classified by q as

- Horizontal trajectory: $f(\gamma(t))\dot{\gamma}(t)^2 > 0$;
- Vertical trajectory: $f(\gamma(t))\dot{\gamma}(t)^2 < 0$.

Locally, one can find coordinates so that horizontal trajectories look like concentric circles while vertical trajectories look like rays emanating from a single point.

Then we can define the *Strebel differential*:

Definition 2.3. *For a Riemann surface X of genus $g \geq 0$ with $n \geq 1$ marked points $\{p_1, \dots, p_n\}$ such that $2 - 2g < n$, and a given n -tuple $a_{i=1, \dots, n} \in \mathbb{R}^+$, a Strebel differential $q = f(z)dz^2$ is a quadratic differential such that*

- f is holomorphic on $X \setminus \{p_1, \dots, p_n\}$;
- f has a second-order pole at each p_i ;
- the union of all non-compact horizontal trajectories of q is a closed subset of X of measure 0;

- every compact horizontal of q is a simple loop A centered at p_i such that $a_i = \oint_{A_i} \sqrt{q}$. (Here the branch of the square root is chosen so that the integral has a positive value with respect to the positive orientation of A_i that is determined by the complex structure of X .)

The upshot is that [37]

Theorem 2.2. *The Strebel differential is the pull-back, by a Belyi map $\beta : X \rightarrow \mathbb{P}^1$, of a quadratic differential on \mathbb{P}^1 with 3 punctures,*

$$q = \beta^* \left(\frac{d\zeta^2}{4\pi^2\zeta(1-\zeta)} \right) = \frac{(d\beta)^2}{4\pi^2\beta(1-\beta)} = \frac{(\beta')^2}{4\pi^2\beta(1-\beta)} dz^2, \quad (2.55)$$

where z and ζ are coordinates on X and \mathbb{P}^1 respectively.

Recall the definition of the SW differential [30]

$$\lambda = x \frac{dz}{z}. \quad (2.56)$$

Then

$$q = \lambda^2 = x^2 \frac{dz^2}{z^2} =: \phi(z) dz^2 \quad (2.57)$$

is the quadratic differential on \mathcal{C} . For our purposes, the important point to note is that the SW curve (2.34) can be written in the form (2.57) [30]. This construction will prove essential in what follows.

SW curves and Dessins As mentioned above, the SW curve Σ is related to the quadratic differential q . Moving in the moduli space of the theory in question will alter the parameters in the SW curve, thereby altering the parameters in q [9]. Following [37], it was found in [9] that at certain isolated points in the Coulomb branch $\mathcal{U}_{g,n}$, where g is the genus of the Gaiotto curve \mathcal{C} with n marked points, q is completely fixed and becomes a Strebel differential $q = \phi(t) dt^2 = \frac{d\beta^2}{4\pi^2\beta(t)(1-\beta(t))}$.

For $SU(2)$ with $N_f = 4$, there exists 6 such Strebel points in $\mathcal{U}_{g,n} \times \mathbb{R}^n$, for which the Belyi maps are presented in Table 2.1. Here, the astute readers will recognise the striking fact that these six Belyi maps are those found in [7, 38] to be associated to the six *genus zero, torsion-free, congruence* subgroups of the modular group $\Gamma = \mathrm{PSL}(2, \mathbb{Z}) \cong \mathbb{Z}_2 * \mathbb{Z}_3$, where $*$ denotes the free product⁴.

From the Belyi maps in Table 2.1, we can compute the associated dessins as displayed in Figure 2.2. The dessins d'enfants associated to each Strebel point of the

⁴For the background on the congruence subgroups of Γ , see Appendix C. It remains an open question whether dessins associated to other subgroups of the modular group, perhaps of higher index, arise for other $\mathcal{N} = 2$ generalised quiver theories in a parallel manner.

Graph	$\beta(t)$	Ramification	Strebel q
$\Gamma(3)$	$\frac{t^3(t+6)^3(t^2-6t+36)^3}{1728(t-3)^3(t^2+3t+9)^3}$	$[3^4 2^6 3^4]$	$-\frac{9t(t^3+216)}{4\pi^2(t^3-27)^2}$
$\Gamma_0(4) \cap \Gamma(2)$	$\frac{(t^4+224t^2+256)^3}{1728t^2(t-4)^4(t+4)^4}$	$[3^4 2^6 4^2, 2^2]$	$-\frac{4t^4+896t^2+1024}{4\pi^2t^2(t^2-16)^2}$
$\Gamma_1(5)$	$\frac{(t^4+248t^3+4064t^2+22312t+40336)^3}{1728(t+5)(t^3-t-31)^5}$	$[3^4 2^6 5^2, 1^2]$	$-\frac{t^4+248t^3+4064t^2+22312t+40336}{4\pi^2(t+5)^2(t^2-t-31)^2}$
$\Gamma_0(6)$	$\frac{(t+7)^3(t^3+237t^2+1443t+2287)^3}{1728(t+3)^2(t+4)^3(t-5)^6}$	$[3^4 2^6 6, 3, 2, 1]$	$-\frac{(t+7)(t^3+237t^2+1443t+2287)}{4\pi^2(t+5)^2(t+3)^2(t+4)^2}$
$\Gamma_0(8)$	$\frac{(t^4+240t^3+2144t^2+3840t+256)^3}{1728t(t+4)^2(t-4)^8}$	$[3^4 2^6 8, 2, 1^2]$	$-\frac{t^4+240t^3+2144t^2+3840t+256}{4\pi^2t^2(t^2-16)^2}$
$\Gamma_0(9)$	$\frac{(t+6)^3(t^3+234t^2+756t+2160)^3}{1728(t^2+3t+9)(t-3)^9}$	$[3^4 2^6 9, 1^3]$	$-\frac{(t+6)(t^3+234t^2+756t+2160)}{4\pi^2(t^3-27)^2}$

Table 2.1: The list of the six genus-zero, torsion-free, congruence subgroups of the modular group Γ , of index 12. The corresponding Belyi maps $\beta(t)$ and their ramification indices, as well as the Strebel differentials are also shown. Note that the ramification indices for all 6 are such that there are 4 pre-images of 0 of order 3 and 6 pre-images of 1 of order 2. The pre-images of ∞ (aka the *cuspidal widths*) all add to 12, as do the ramification indices for 0 and 1. This is required by the fact that all the subgroups are of index 12 within Γ .

$$\begin{array}{ccc}
\text{fig/New_3-3-3-3.pdf} & \text{fig/4-4-2-2.pdf} & \text{fig/5-5-1-1.pdf} \\
\Gamma(3) & \Gamma_0(4) \cap \Gamma(2) & \Gamma_1(5) \\
\text{fig/6-3-2-1.pdf} & \text{fig/8-2-1-1.pdf} & \text{fig/New_9-1-1-1.pdf} \\
\Gamma_0(6) & \Gamma_0(8) & \Gamma_0(9)
\end{array}$$

Figure 2.2: The dessins d'enfants associated to the six Strebel points of the $SU(2)$, $N_f = 4$ theory.

generalised quiver theory in question turn out to have an interpretation as so-called *ribbon graphs* on the Gaiotto curve \mathcal{C} . For details, the readers are referred to [9, 37].

3 From Dessins to Conformal Blocks

Let us now complete the cycle of the route map above by considering what gauge theory and CFT data we can obtain starting from the 6 dessins.

3.1 The $SU(2)$ with 4 Flavours

Given that all our graphs in Figure 2.2 are drawn on the Riemann surface (genus zero) with 4 marked points (one for each face), we can naturally interpret these as Gaiotto curves [6, 9], and thence $\mathcal{N} = 2$ gauge theories.

To begin, the Seiberg-Witten curve Σ for the $SU(2)$ $N_f = 4$ theory in algebraic form is standard [30]. For future convenience, we start with the SW curve of form

(2.50) and write the SW differential as [13]

$$\lambda_{SW} = \frac{\sqrt{P_4(z)}}{z(z-1)(z-\zeta)} dz, \quad P_4(z) = m_0^2 \prod_{i=1}^4 (z - \lambda_i) = m_0^2 \sum_{i=0}^4 z^{4-i} S_i, \quad (3.1)$$

under the substitution

$$\begin{aligned} \lambda_{SW} &= v/z, \quad t = z, \quad q = \zeta, \\ \mu_1 &= m_1 + m_3, \quad \mu_2 = m_1 - m_3, \quad \mu_3 = m_2 + m_0, \quad \mu_4 = m_2 - m_0, \end{aligned} \quad (3.2)$$

where U is proportional to the moduli parameter u with coefficient only depending on the UV gauge coupling $q = \zeta$ [14]. The parameters S_i are given in terms of the flavour mass and coupling parameters $m_{0,1,2,3}, \zeta, U \in \mathbb{C}$ so that $S_0 = 1$ for the top coefficient and

$$\begin{aligned} m_0^2 S_1 &= - (m_0^2 + m_2^2(\zeta - 1) + m_0^2 \zeta + 2m_2 m_3 \zeta + (1 + \zeta)U), \\ m_0^2 S_2 &= (m_0^2 + m_1^2 - m_3^2 + 2m_2 m_3) \zeta + m_2^2(\zeta - 1) \zeta + 2m_2 m_3 \zeta^2 + m_3^2 \zeta^2 + (1 + \zeta)^2 U, \\ m_0^2 S_3 &= - ((m_1^2 - m_3^2) \zeta + (m_1^2 + 2m_2 m_3 + m_3^2) \zeta^2 + \zeta(1 + \zeta)U), \\ m_0^2 S_4 &= m_1^2 \zeta^2. \end{aligned} \quad (3.3)$$

On the other hand, the S -parameters can be written in terms of the λ_i as standard symmetric polynomials,

$$S_k = \sum_{1 \leq j_1 \leq \dots \leq j_k \leq 4} \lambda_{j_1} \dots \lambda_{j_k}. \quad (3.4)$$

The periods can be obtained by prepotential methods with which [13] nicely determined,

$$\frac{da(U)}{dU} = -\frac{1}{\pi i} \frac{1 + \zeta}{m_0 \sqrt{(\lambda_2 - \lambda_3)(\lambda_1 - \lambda_4)}} K(r^2), \quad (3.5)$$

where

$$r^2 = \frac{(\lambda_1 - \lambda_2)(\lambda_3 - \lambda_4)}{(\lambda_1 - \lambda_3)(\lambda_2 - \lambda_4)}, \quad (3.6)$$

and

$$K(x) := \int_0^{\pi/2} \frac{d\theta}{\sqrt{1 - x^2 \sin^2 \theta}} \quad (3.7)$$

is the elliptic integral of the first kind. The right hand side of (3.5) implicitly depends on U , through λ_i and thence S_i , thus we only need to integrate (indefinitely) it to obtain $a(U)$ as a function of U , which could be a daunting task analytically.

Let us nevertheless attempt at some simplifications. First, we see that the right hand side depends only on the three cross-terms in the four λ_i , which we will denote as

$\lambda_{(23)(14)}$, $\lambda_{(12)(34)}$ and $\lambda_{(13)(24)}$, with r^2 being a cross-ratio in the second and the third. Combining with (3.4), let us see whether these can be directly expressed in terms of S_i , and thence, in terms of U . This is a standard algebraic elimination problem and we readily find the following:

Lemma 3.1. *Consider the monic cubic polynomial $\mathcal{C}(x)$,*

$$\begin{aligned} x^3 &+ (-2S_2^2 + 6S_1S_3 - 24S_4) x^2 + (S_2^4 - 6S_1S_3S_2^2 + 24S_4S_2^2 + 9S_1^2S_3^2 + 144S_4^2 - 72S_1S_3S_4) x \\ &+ 27S_4^2S_1^4 + 4S_3^3S_1^3 - 18S_2S_3S_4S_1^3 - 144S_2S_4^2S_1^2 + 4S_2^3S_4S_1^2 + 6S_3^2S_4S_1^2 - 18S_2S_3^3S_1 + 192S_3S_4^2S_1 \\ &+ 80S_2^2S_3S_4S_1 + 27S_3^4 - 256S_4^3 + 4S_2^3S_3^2 - S_1^2S_2^2S_3^2 + 128S_2^2S_4^2 - 16S_2^4S_4 - 144S_2S_3^2S_4. \end{aligned} \quad (3.8)$$

The squares of the 3 cross-products

$$x_1 = \lambda_{(12)(34)}^2, \quad x_2 = \lambda_{(23)(14)}^2, \quad x_3 = \lambda_{(13)(24)}^2; \quad \lambda_{(ij)(mn)} := (\lambda_i - \lambda_j)(\lambda_m - \lambda_n) \quad (3.9)$$

are the three roots of $\mathcal{C}(x)$.

Of course, we can substitute the S_i parameters in terms of the m_i, ζ, U parameters from (3.1), though the expression become too long to present here. Each of x_1, x_2 and x_3 can be solved from the cubic $\mathcal{C}(x)$, which then places each as a function of U explicitly by substituting the expressions of S_i in (3.3). Then, we have $a(U)$ as the anti-derivative

$$a(U) = -\frac{1 + \zeta}{m_0\pi i} \int_0^U \frac{dU_0}{\sqrt[4]{\tilde{x}_2(U_0)}} K \left(\frac{\sqrt{\tilde{x}_1(U_0)}}{\sqrt{\tilde{x}_3(U_0)}} \right), \quad (3.10)$$

where we have marked \tilde{x}_i explicitly as U -dependent, in addition to depending on the parameters ζ and m_i . As $a \sim \sqrt{u}$ and $U \sim u$, we should have $a(0) = 0$. Here \tilde{x} indicates that the above is sketchy since there could be (at most) six distinct solutions as in Table 3.1.

$\sqrt{\tilde{x}_1}$	$\sqrt{\tilde{x}_2}$	$\sqrt{\tilde{x}_3}$
$\sqrt{x_1}$	$\sqrt{x_2}$	$\sqrt{x_3}$
$-\sqrt{x_1}$	$\sqrt{x_3}$	$\sqrt{x_2}$
$\sqrt{x_3}$	$-\sqrt{x_2}$	$\sqrt{x_1}$
$-\sqrt{x_3}$	$\sqrt{x_1}$	$-\sqrt{x_2}$
$\sqrt{x_2}$	$-\sqrt{x_3}$	$-\sqrt{x_1}$
$-\sqrt{x_2}$	$-\sqrt{x_1}$	$-\sqrt{x_3}$

Table 3.1: The possible combinations of x_i 's in $a(U)$.

Recall the definition of the Seiberg-Witten differential from (2.57), we have that

$$\lambda_{\text{SW}}^2 = \phi_{\text{SW}}(z) dz^2 \quad (3.11)$$

is a quadratic differential. This is the above mentioned meromorphic quadratic differential on \mathcal{C} . Moving in the moduli space of the theory in question will alter the parameters in the Seiberg-Witten curve, thereby altering the parameters in q (cf. [9]). Following [37], it was found in [9] that at certain isolated points in the Coulomb branch of the moduli space $\mathcal{U}_{g,n}$ of the gauge theory in question, where g is the genus of the Gaiotto curve \mathcal{C} with n marked points, q is completely fixed, which becomes a Strebel differential.

We therefore have two forms of the Strebel differentials, $\phi_\beta(t)$ coming from the dessin and $\phi_{\text{SW}}(z)$ coming from the physics. Now, because dessins are *rigid*, they have no parameters. The insight of Belyi and Grothendieck is precisely that the map β have parameters fixed at very special algebraic points in moduli space. Thus, $\phi_\beta(t)$ is of a particular form, as a rational function in t and fixed algebraic coefficients.

On the other hand $\phi_{\text{SW}}(z)$ from the gauge theory has parameters which we saw earlier, corresponding to masses, couplings etc. Therefore, up to redefinition of the variables (t, z) and identifying $\phi_{\text{SW}}(z)$ and $\phi_\beta(t)$ it is natural to ask how the special values of the parameters from the dessin perspective *fix* the physical parameters in the gauge theory.

We have now introduced all the necessary dramatis personae of our tale and our strategy is thus clear. There are also some further details that we should be careful about in the calculations. We will work through an example in detail to illustrate them in the following subsection.

3.2 Example: $\Gamma(3)$

Let us take the dessin for $\Gamma(3)$, whose Belyi map is

$$\beta(t) = \frac{t^3(t+6)^3(t^2-6t+36)^3}{1728(t-3)^3(t^2+3t+9)^3}. \quad (3.12)$$

We can readily get the pre-images of 0, 1 and ∞ :

	Pre-image	Ramification
$\beta^{-1}(0)$	-6	3
	0	3
	$3 - 3i\sqrt{3}$	3
	$3 + 3i\sqrt{3}$	3
$\beta^{-1}(1)$	$3(1 - \sqrt{3})$	2
	$3(1 + \sqrt{3})$	2
	$(\frac{3}{2} + \frac{3i}{2})(\sqrt{3} + (-2 - i))$	2
	$(-\frac{3}{2} - \frac{3i}{2})(\sqrt{3} + (2 + i))$	2
	$\frac{1}{2}((-3 + 9i) - (3 - 3i)\sqrt{3})$	2
	$\frac{1}{2}((-3 + 9i) + (3 - 3i)\sqrt{3})$	2
$\beta^{-1}(\infty)$	∞	3
	3	3
	$-\frac{3}{2}i(\sqrt{3} - i)$	3
	$\frac{3}{2}i(\sqrt{3} + i)$	3

We can construct the corresponding dessin as in Figure 2.2. Subsequently, using (2.55), we see that the Strebel differential is $q = \phi_\beta(t)dt^2$, where

$$\phi_\beta(t) = -\frac{9t(t^3 + 216)}{4\pi^2(t^3 - 27)^2}. \quad (3.14)$$

We have marked ϕ with a subscript β to emphasize its dessin origin. On the other side, we have the Seiberg-Witten curve and quadratic differential for $SU(2)$ with $N_f = 4$ from (3.1) and (3.11), to be

$$\begin{aligned} \phi_{\text{sw}}(z) &= \frac{P_4(z)}{(z(z-1)(z-\zeta))^2}, \quad \text{where} \\ P_4(z) &= z^4 m_0^2 - z^3 (m_0^2 + m_2^2(\zeta - 1) + m_0^2 \zeta + 2m_2 m_3 \zeta + (1 + \zeta)U) \\ &\quad + z^2 ((m_0^2 + m_1^2 - m_3^2 + 2m_2 m_3)\zeta + m_2^2(\zeta - 1)\zeta + 2m_2 m_3 \zeta^2 + m_3^2 \zeta^2 + (1 + \zeta)^2 U) \\ &\quad - z ((m_1^2 - m_3^2)\zeta + (m_1^2 + 2m_2 m_3 + m_3^2)\zeta^2 + \zeta(1 + \zeta)U) + m_1^2 \zeta^2. \end{aligned} \quad (3.15)$$

Here, likewise we have marked ϕ with a subscript ‘‘SW’’ to emphasize its Seiberg-Witten origin. We have also explicitly written the differential coming from the Seiberg-Witten side in terms of the parameters $m_{0,1,2,3}, \zeta, U$.

We need to match (3.14) with (3.15), up to an $\text{PGL}(2, \mathbb{C})$ transformation on the complex variable z . The reason for this is that we are dealing in this example with

a quadratic differential on the *sphere*. For curves of higher genus, such $\text{PGL}(2, \mathbb{C})$ transformations are generically not permitted, as they will not preserve the structure of the poles and zeroes of the quadratic differential.

We can therefore write⁵

$$z = \frac{at + b}{ct + d}, \quad a, b, c, d \in \mathbb{C} \quad (3.16)$$

and solve for complex coefficients a, b, c, d as well as the parameters $m_{0,1,2,3}, \zeta, U$ so that we have identically for all t that

$$\phi_\beta(t) = \phi_{\text{SW}} \left(\frac{at + b}{ct + d} \right). \quad (3.17)$$

There are actually continuous families of 2×2 matrices solving this equation for a given dessin. As the elliptic curve is the same up to an overall factor, it turns out that each continuous family would simply scale the SW differential by $\phi_{\text{SW}} \rightarrow k^2 \phi_{\text{SW}}$ with $k \in \mathbb{R}$. Obviously, equating the numerators of ϕ_β and ϕ_{SW} as well as equating their denominators would give a solution. For future convenience, such solution will be referred to as the “basic” values of the parametrization. Then other parametrizations would simply follow

$$\phi_{\text{SW}} = \pm k^2 \phi_{\text{SW, basic}}. \quad (3.18)$$

There are two points we should pay attention to:

- Here, we simply insist on CFTs that can be formulated on the torus, that is, their partition functions on the torus are modular invariant. Then we can only allow primary states with pure imaginary charges. Recall the AGT relation (2.20), which in terms of m_i is

$$\begin{aligned} m'_0 + Q = \alpha_4, \quad m'_1 = \alpha_1, \quad m'_2 = \alpha_3, \quad m'_3 + Q = \alpha_2, \quad m'_i = \frac{m_i - (\epsilon_1 + \epsilon_2)/2}{\sqrt{\epsilon_1 \epsilon_2}} \\ \frac{a}{\sqrt{\epsilon_1 \epsilon_2}} + \frac{Q}{2} = \alpha_{\text{int}}, \quad e^{2\pi i \tau} = \zeta, \quad \frac{-\sum_i m_i + 2(\epsilon_1 + \epsilon_2)}{\sqrt{\epsilon_1 \epsilon_2}} = \sum_i \alpha_i = Q, \end{aligned} \quad (3.19)$$

where we have included the factor $1/\sqrt{\epsilon_1 \epsilon_2}$ and the shift of $(\epsilon_1 + \epsilon_2)/2$ as discussed in Appendix A. In fact, $\epsilon_{1,2}$ are not completely free since $Q = (\epsilon_1 + \epsilon_2)/\sqrt{\epsilon_1 \epsilon_2}$. Therefore,

$$\sum_i m_i = \epsilon_1 + \epsilon_2. \quad (3.20)$$

⁵Some algebra shows that the transformation should always satisfy $z = (at + b)/d$, i.e., a linear transformation.

Hence, we also have

$$\frac{1}{\sqrt{\epsilon_1 \epsilon_2}} \sum_i m_i = Q. \quad (3.21)$$

In other words, only real or pure imaginary m_i 's, based on the sign of $\epsilon_1 \epsilon_2$, are allowed. Hence, there is a “ \pm ” on the right hand side. Furthermore, we find that Q does not see the shift except a sign change (compared to no shifts). In particular, Q is not affected by the shift when it is zero, i.e., $\epsilon_1 = -\epsilon_2$.

- There is also a coefficient k^2 on the right hand side, where k being real follows the same reasoning as the \pm sign. One may easily check that an SW differential/elliptic curve would have the same j -invariant under $\phi \rightarrow k^2 \phi$. As a result, the parameters, by looking at $P_4(z)$ and $a(U)$, would follow

$$\begin{aligned} \zeta &\rightarrow \zeta, \quad m_i \rightarrow k m_i, \quad a \rightarrow k a, \quad U \rightarrow k^2 U; \\ \alpha_{i,\text{int}} &\rightarrow k \alpha_{i,\text{int}}, \quad Q \rightarrow k Q. \end{aligned} \quad (3.22)$$

Therefore, rather than discrete parameters, we would have *families* of differentials. Importantly, we can see that the coupling ζ is *invariant* (and so is Q when we have $c = 1$ CBs).

Now expanding the above and setting all the coefficients of t to vanish identically gives a complicated polynomial system in $(a, b, c, d, m_{0,1,2,3}, \zeta, U)$ for which one can find many solutions. For example, the following constitutes a solution (with $k = 1$),

$$m_0 = -m_1 = m_2 = -m_3 = \frac{1}{2\sqrt{3}\pi}, \quad \zeta = \frac{1}{2} + \frac{i\sqrt{3}}{2}, \quad U = \frac{1}{9\pi^2} \quad (3.23)$$

with $(a, b, c, d) = \left(\frac{1+i}{\sqrt{2}3^{3/4}}, i \left(\frac{\sqrt{3}}{2\sqrt{2}} - \frac{3^{3/4}}{2\sqrt{2}} \right) + \frac{\sqrt{3}}{2\sqrt{2}} + \frac{3^{3/4}}{2\sqrt{2}}, 0, \frac{(1-i)3^{3/4}}{\sqrt{2}} \right)$, which are not so important. With the parameters (3.23) as fixed, the numerator of the SW differential takes the form

$$P_4(z) = -\frac{6z^4 - 4i(\sqrt{3} - 3i)z^3 + (6 + 6i\sqrt{3})z^2 - 8i\sqrt{3}z + 3i\sqrt{3} - 3}{72\pi^2}. \quad (3.24)$$

We now need the roots λ_i of $P_4(z)$ as given in (3.1):

$$z^4 + \left(-2 - \frac{2i}{\sqrt{3}} \right) z^3 + \left(1 + i\sqrt{3} \right) z^2 - \frac{4i}{\sqrt{3}} z + \frac{1}{2} i \left(\sqrt{3} + i \right) = \prod_{i=1}^4 (z - \lambda_i). \quad (3.25)$$

The SW curve itself is genus 1 and is in fact an elliptic curve. We can recast (3.15) into hyper-elliptic form as

$$\begin{aligned} y^2 = & z^4 m_0^2 - z^3 (m_0^2 + m_2^2(\zeta - 1) + m_0^2 \zeta + 2m_2 m_3 \zeta + (1 + \zeta)U) \\ & + z^2 ((m_0^2 + m_1^2 - m_3^2 + 2m_2 m_3)\zeta + m_2^2(\zeta - 1)\zeta + 2m_2 m_3 \zeta^2 + m_3^2 \zeta^2 + (1 + \zeta)^2 U) \\ & - z ((m_1^2 - m_3^2)\zeta + (m_1^2 + 2m_2 m_3 + m_3^2)\zeta^2 + \zeta(1 + \zeta)U) + m_1^2 \zeta^2, \end{aligned} \quad (3.26)$$

where the redefinition $y^2 = (z(z - 1)(z - \zeta))^2 \phi_{\text{SW}}(z) = P_4(z)$ is used. Following Appendix D, as one may check, the j -invariant we get from the parameterization (3.23) agrees with the one directly from the Strebel differential (3.14):

$$j = 0. \quad (3.27)$$

Indeed, $j = 0$ corresponds to a special elliptic curve with $\mathbb{Z}/3\mathbb{Z}$ -symmetry, much like the dessin for $\Gamma(3)$ itself.

In this case, we can integrate (3.10) numerically to obtain

$$a(U) = \pm 0.19055 + 0.287317i, \quad \pm 0.00292968 + 0.00493721i, \quad -0.0171. \quad (3.28)$$

Now we can use the AGT relation (3.19) to get the parametrizations for CBs. Recall that the α 's should have vanishing real parts. Therefore, we would only keep the pure imaginary value for a . Together with $\sum_i \alpha_i = Q$, we have

$$Q = 0, \quad \alpha_1 = \alpha_2 = -\alpha_3 = -\alpha_4 = \frac{i}{2\sqrt{3}\pi}, \quad \alpha_{\text{int}} = 0.0171i, \quad e^{2\pi i \tau} = \frac{1}{2} + \frac{i\sqrt{3}}{2}, \quad (3.29)$$

where we have taken $\epsilon_1 = -\epsilon_2 = 1$ for simplicity as $\epsilon_1 + \epsilon_2 = 0$ here.

Since the mass parameters and the deformation parameters should always be both real or pure imaginary such that the CFT parameters would be pure imaginary, we can also have pure imaginary m_i 's and a for the above example, viz,

$$m_0 = -m_1 = m_2 = -m_3 = \frac{i}{2\sqrt{3}\pi}, \quad \zeta = \frac{1}{2} + \frac{i\sqrt{3}}{2}, \quad U = -\frac{1}{9\pi^2}, \quad a = -0.171i. \quad (3.30)$$

Then we can still get the same CFT parameters as in (3.29) with the choice⁶ $\epsilon_1 = -\epsilon_2 = i$.

In general, $\pm k^2 \phi_{\text{SW, basic}}$ with a fixed k would give two types of solutions with one real and the other imaginary as the corresponding CFT parameters should be pure

⁶It should still be allowed to have imaginary deformation parameters as in terms of the B-model, $s = (\epsilon_1 + \epsilon_2)^2$ and $g_s = (\epsilon_1 \epsilon_2)^2$ would still be real (where physically the power of s in the holomorphic anomaly equation counts the number of insertions of an operator [39]).

imaginary. Both of them give the same CFT data. These two types of solutions are simply related by⁷

$$m_{i,\text{imaginary}} = im_{i,\text{real}}, \quad a_{\text{imaginary}} = ia_{\text{real}}, \quad \zeta_{\text{imaginary}} = \zeta_{\text{real}}, \quad U_{\text{imaginary}} = -U_{\text{real}}, \quad (3.31)$$

where the subscripts for ζ and U are only used to indicate whether their corresponding m_i and a are real or pure imaginary (rather than themselves).

3.3 Matching Parameters

Here, we report all parameters from the six dessins in Table 3.2~3.7. Notice that we are only giving solutions coming from $(\pm)\phi_{\text{SW,basic}}$. There is actually a family for each parametrization following (3.22). In particular, we are only giving the pure imaginary m_i 's and a , and there should be a similar set of (real) solutions in terms of (3.31).

$\zeta = e^{2\pi i\tau}$	m_0	m_1	m_2	m_3	U	$\sqrt{\epsilon_1\epsilon_2}Q$	$a = \frac{\alpha_{\text{int}}}{\sqrt{\epsilon_1\epsilon_2}} + \frac{Q}{2}$
$\frac{1}{2}(1 - i\sqrt{3})$	$-\frac{i}{2\sqrt{3}\pi}$	$-\frac{i}{2\sqrt{3}\pi}$	$\frac{i}{2\sqrt{3}\pi}$	$-\frac{i}{2\sqrt{3}\pi}$	$-\frac{1}{9\pi^2}$	$-\frac{i}{\sqrt{3}\pi}$	$-0.0171i$
	$-\frac{i}{2\sqrt{3}\pi}$	$\frac{i}{2\sqrt{3}\pi}$	$-\frac{i}{2\sqrt{3}\pi}$	$\frac{i}{2\sqrt{3}\pi}$	$-\frac{1}{9\pi^2}$	0	$-0.0171i$
	$\frac{i}{2\sqrt{3}\pi}$	$-\frac{i}{2\sqrt{3}\pi}$	$\frac{i}{2\sqrt{3}\pi}$	$-\frac{i}{2\sqrt{3}\pi}$	$-\frac{1}{9\pi^2}$	0	$0.0171i$
	$\frac{i}{2\sqrt{3}\pi}$	$\frac{i}{2\sqrt{3}\pi}$	$-\frac{i}{2\sqrt{3}\pi}$	$\frac{i}{2\sqrt{3}\pi}$	$-\frac{1}{9\pi^2}$	$\frac{i}{\sqrt{3}\pi}$	$0.0171i$
$\frac{1}{2}(1 + i\sqrt{3})$	$-\frac{i}{2\sqrt{3}\pi}$	$-\frac{i}{2\sqrt{3}\pi}$	$\frac{i}{2\sqrt{3}\pi}$	$-\frac{i}{2\sqrt{3}\pi}$	$-\frac{1}{9\pi^2}$	$-\frac{i}{\sqrt{3}\pi}$	$0.0171i$
	$-\frac{i}{2\sqrt{3}\pi}$	$\frac{i}{2\sqrt{3}\pi}$	$-\frac{i}{2\sqrt{3}\pi}$	$\frac{i}{2\sqrt{3}\pi}$	$-\frac{1}{9\pi^2}$	0	$0.0171i$
	$\frac{i}{2\sqrt{3}\pi}$	$-\frac{i}{2\sqrt{3}\pi}$	$\frac{i}{2\sqrt{3}\pi}$	$-\frac{i}{2\sqrt{3}\pi}$	$-\frac{1}{9\pi^2}$	0	$-0.0171i$
	$\frac{i}{2\sqrt{3}\pi}$	$\frac{i}{2\sqrt{3}\pi}$	$-\frac{i}{2\sqrt{3}\pi}$	$\frac{i}{2\sqrt{3}\pi}$	$-\frac{1}{9\pi^2}$	$\frac{i}{\sqrt{3}\pi}$	$-0.0171i$

Table 3.2: The parameters obtained from $\Gamma(3)$. Using (3.19), we can get the values for α_i 's.

$\zeta = e^{2\pi i\tau}$	m_0	m_1	m_2	m_3	U	$\sqrt{\epsilon_1\epsilon_2}Q$	a
	$-\frac{i}{8\pi}$	$-\frac{i}{4\pi}$	$-\frac{i}{4\pi}$	$-\frac{i}{8\pi}$	$-\frac{1}{192\pi^2}$	$-\frac{3i}{4\pi}$	$-0.0046i$
							$-0.0061i$
	$\frac{i}{8\pi}$	$-\frac{i}{4\pi}$	$-\frac{i}{4\pi}$	$-\frac{i}{8\pi}$	$-\frac{1}{192\pi^2}$	$-\frac{i}{2\pi}$	$0.0046i$
							$0.0061i$

⁷For those discarded a 's which are not real/pure imaginary, they actually satisfy this relation as well.

$\frac{1}{2}$

$-\frac{i}{8\pi}$	$-\frac{i}{4\pi}$	$-\frac{i}{4\pi}$	$\frac{i}{8\pi}$	$-\frac{3}{64\pi^2}$	$-\frac{i}{2\pi}$	$-0.0409i$ $-0.0478i$
$-\frac{i}{8\pi}$	$\frac{i}{4\pi}$	$-\frac{i}{4\pi}$	$-\frac{i}{8\pi}$	$-\frac{1}{192\pi^2}$	$-\frac{i}{4\pi}$	$-0.0046i$ $-0.0061i$
$\frac{i}{8\pi}$	$-\frac{i}{4\pi}$	$-\frac{i}{4\pi}$	$\frac{i}{8\pi}$	$-\frac{3}{64\pi^2}$	$-\frac{i}{4\pi}$	$0.0409i$ $0.0478i$
$-\frac{i}{8\pi}$	$-\frac{i}{4\pi}$	$\frac{i}{4\pi}$	$-\frac{i}{8\pi}$	$-\frac{3}{64\pi^2}$	$-\frac{i}{4\pi}$	$-0.0409i$ $-0.0478i$
$\frac{i}{8\pi}$	$\frac{i}{4\pi}$	$-\frac{i}{4\pi}$	$-\frac{i}{8\pi}$	$-\frac{1}{192\pi^2}$	0	$0.0046i$ $0.0061i$
$-\frac{i}{8\pi}$	$\frac{i}{4\pi}$	$-\frac{i}{4\pi}$	$\frac{i}{8\pi}$	$-\frac{3}{64\pi^2}$	0	$-0.0409i$ $-0.0478i$
$\frac{i}{8\pi}$	$-\frac{i}{4\pi}$	$\frac{i}{4\pi}$	$-\frac{i}{8\pi}$	$-\frac{3}{64\pi^2}$	0	$0.0409i$ $0.0478i$
$-\frac{i}{8\pi}$	$-\frac{i}{4\pi}$	$\frac{i}{4\pi}$	$\frac{i}{8\pi}$	$-\frac{1}{192\pi^2}$	0	$-0.0046i$ $-0.0061i$
$\frac{i}{8\pi}$	$\frac{i}{4\pi}$	$-\frac{i}{4\pi}$	$\frac{i}{8\pi}$	$-\frac{3}{64\pi^2}$	$\frac{i}{4\pi}$	$0.0409i$ $0.0478i$
$-\frac{i}{8\pi}$	$\frac{i}{4\pi}$	$\frac{i}{4\pi}$	$-\frac{i}{8\pi}$	$-\frac{3}{64\pi^2}$	$\frac{i}{4\pi}$	$-0.0409i$ $-0.0478i$
$\frac{i}{8\pi}$	$-\frac{i}{4\pi}$	$\frac{i}{4\pi}$	$\frac{i}{8\pi}$	$-\frac{1}{192\pi^2}$	$\frac{i}{4\pi}$	$0.0046i$ $0.0061i$
$\frac{i}{8\pi}$	$\frac{i}{4\pi}$	$\frac{i}{4\pi}$	$-\frac{i}{8\pi}$	$-\frac{3}{64\pi^2}$	$\frac{i}{2\pi}$	$0.0409i$ $0.0478i$
$-\frac{i}{8\pi}$	$\frac{i}{4\pi}$	$\frac{i}{4\pi}$	$\frac{i}{8\pi}$	$-\frac{1}{192\pi^2}$	$\frac{i}{2\pi}$	$-0.0046i$ $-0.0061i$
$\frac{i}{8\pi}$	$\frac{i}{4\pi}$	$\frac{i}{4\pi}$	$\frac{i}{8\pi}$	$-\frac{1}{192\pi^2}$	$\frac{3i}{4\pi}$	$0.0046i$ $0.0061i$
$-\frac{i}{4\pi}$	$-\frac{i}{2\pi}$	$-\frac{i}{4\pi}$	$-\frac{i}{2\pi}$	$\frac{1}{6\pi^2}$	$-\frac{3i}{2\pi}$	$0.0731i$ $0.0868i$
$\frac{i}{4\pi}$	$-\frac{i}{2\pi}$	$-\frac{i}{4\pi}$	$-\frac{i}{2\pi}$	$\frac{1}{6\pi^2}$	$-\frac{i}{\pi}$	$-0.0731i$

2

						$-0.0868i$
$-\frac{i}{4\pi}$	$-\frac{i}{2\pi}$	$\frac{i}{4\pi}$	$-\frac{i}{2\pi}$	$-\frac{1}{6\pi^2}$	$-\frac{i}{\pi}$	$-0.0731i$ $-0.0868i$
$\frac{i}{4\pi}$	$-\frac{i}{2\pi}$	$\frac{i}{4\pi}$	$-\frac{i}{2\pi}$	$-\frac{1}{6\pi^2}$	$-\frac{i}{2\pi}$	$0.0731i$ $0.0868i$
$-\frac{i}{4\pi}$	$-\frac{i}{2\pi}$	$-\frac{i}{4\pi}$	$\frac{i}{2\pi}$	$-\frac{1}{6\pi^2}$	$-\frac{i}{2\pi}$	$-0.0731i$ $-0.0868i$
$-\frac{i}{4\pi}$	$\frac{i}{2\pi}$	$-\frac{i}{4\pi}$	$-\frac{i}{2\pi}$	$\frac{1}{6\pi^2}$	$-\frac{i}{2\pi}$	$0.0731i$ $0.0868i$
$\frac{i}{4\pi}$	$\frac{i}{2\pi}$	$-\frac{i}{4\pi}$	$-\frac{i}{2\pi}$	$\frac{1}{6\pi^2}$	0	$-0.0731i$ $-0.0868i$
$-\frac{i}{4\pi}$	$\frac{i}{2\pi}$	$\frac{i}{4\pi}$	$-\frac{i}{2\pi}$	$-\frac{1}{6\pi^2}$	0	$-0.0731i$ $-0.0868i$
$\frac{i}{4\pi}$	$-\frac{i}{2\pi}$	$-\frac{i}{4\pi}$	$\frac{i}{2\pi}$	$-\frac{1}{6\pi^2}$	0	$0.0731i$ $0.0868i$
$-\frac{i}{4\pi}$	$-\frac{i}{2\pi}$	$\frac{i}{4\pi}$	$\frac{i}{2\pi}$	$\frac{1}{6\pi^2}$	0	$0.0731i$ $0.0868i$
$\frac{i}{4\pi}$	$-\frac{i}{2\pi}$	$\frac{i}{4\pi}$	$\frac{i}{2\pi}$	$\frac{1}{6\pi^2}$	$\frac{i}{2\pi}$	$-0.0731i$ $-0.0868i$
$\frac{i}{4\pi}$	$\frac{i}{2\pi}$	$\frac{i}{4\pi}$	$-\frac{i}{2\pi}$	$-\frac{1}{6\pi^2}$	$\frac{i}{2\pi}$	$0.0731i$ $0.0868i$
$-\frac{i}{4\pi}$	$\frac{i}{2\pi}$	$-\frac{i}{4\pi}$	$\frac{i}{2\pi}$	$-\frac{1}{6\pi^2}$	$\frac{i}{2\pi}$	$-0.0731i$ $-0.0868i$
$\frac{i}{4\pi}$	$\frac{i}{2\pi}$	$-\frac{i}{4\pi}$	$\frac{i}{2\pi}$	$-\frac{1}{6\pi^2}$	$\frac{i}{\pi}$	$0.0731i$ $0.0868i$
$-\frac{i}{4\pi}$	$\frac{i}{2\pi}$	$\frac{i}{4\pi}$	$\frac{i}{2\pi}$	$\frac{1}{6\pi^2}$	$\frac{i}{\pi}$	$0.0731i$ $0.0868i$
$\frac{i}{4\pi}$	$\frac{i}{2\pi}$	$\frac{i}{4\pi}$	$\frac{i}{2\pi}$	$\frac{1}{6\pi^2}$	$\frac{3i}{2\pi}$	$-0.0731i$ $-0.0868i$
$-\frac{i}{4\pi}$	$-\frac{i}{4\pi}$	$-\frac{i}{2\pi}$	$\frac{i}{2\pi}$		$-\frac{i}{2\pi}$	
$-\frac{i}{4\pi}$	$-\frac{i}{4\pi}$	$\frac{i}{2\pi}$	$-\frac{i}{2\pi}$		$-\frac{i}{2\pi}$	

-1	$\frac{i}{4\pi}$	$-\frac{i}{4\pi}$	$-\frac{i}{2\pi}$	$\frac{i}{2\pi}$	Any value ⁸	0	0
	$\frac{i}{4\pi}$	$-\frac{i}{4\pi}$	$\frac{i}{2\pi}$	$-\frac{i}{2\pi}$		0	
	$-\frac{i}{4\pi}$	$\frac{i}{4\pi}$	$-\frac{i}{2\pi}$	$\frac{i}{2\pi}$		0	
	$-\frac{i}{4\pi}$	$\frac{i}{4\pi}$	$\frac{i}{2\pi}$	$-\frac{i}{2\pi}$		0	
	$\frac{i}{4\pi}$	$\frac{i}{4\pi}$	$-\frac{i}{2\pi}$	$\frac{i}{2\pi}$		$\frac{i}{2\pi}$	
	$\frac{i}{4\pi}$	$\frac{i}{4\pi}$	$\frac{i}{2\pi}$	$-\frac{i}{2\pi}$		$\frac{i}{2\pi}$	

Table 3.3: The parameters obtained from $\Gamma_0(4) \cap \Gamma(2)$. Using (3.19), we can get the values for α_i 's.

As the size of the table increases, we will give a simplified version for the remaining cases below. For each ζ , there are usually $2^4 = 16$ possibilities for pure imaginary m_i 's (and hence 32 possibilities plus the real ones). For a , as the sign of a only depends on the sign of m_0 , “ \pm ” in a means that a has the same sign as m_0 while “ \mp ” in a indicates that m_0 and a have opposite signs⁹.

$\zeta = e^{2\pi i\tau}$	m_0	m_1	m_2	m_3	U	a
0.008065	$\pm 0.014235i$	$\pm 0.071176i$	$0.071176i$	$0.014235i$	-0.000673	$\pm 0.0103i$
			$-0.071176i$	$-0.014235i$		$\pm 0.0139i$
	$\pm 0.014235i$	$\pm 0.071176i$	$0.071176i$	$-0.014235i$	-0.000706	$\pm 0.0107i$
			$-0.071176i$	$0.014235i$		$\mp 0.0148i$
0.991935	$\pm 0.014235i$	$\pm 0.071176i$	$0.071176i$	$0.014235i$	-0.001287	$\pm 0.0285i$
			$0.071176i$	$-0.014235i$		$\mp 0.0295i$
	$\pm 0.014235i$	$\pm 0.071176i$	$0.071176i$	$-0.014235i$	-0.003305	$\pm 0.0566i$
			$-0.071176i$	$0.014235i$		$\pm 0.0576i$
123.991869	$\pm 1.765055i$	$\pm 8.825277i$	$1.765055i$	$8.825277i$	100.010534	$\pm 4.3371i$
			$-1.765055i$	$-8.825277i$		$\mp 4.7490i$
	$\pm 1.765055i$	$\pm 8.825277i$	$1.765055i$	$-8.825277i$	38.200625	$\mp 7.00202i$

⁸Here, any complex number can be a basic value for U since all the terms of U in $P_4(z)$ contain $(1 + \zeta)$ as well.

⁹Notice that in each row, so as not to be confused with the boxes of $m_{2,3}$, there are no solid line between the two lines in the box of a , meaning that there are two possible values for a out of four for each parametrization. For instance, when $\zeta = 0.008065$ and $U = -0.000673$, if $\text{sign}(m_0, m_1, m_2, m_3) = (\pm, \pm, +, +)$, then a can be $0.01025i$ or 0.01391 .

			$-1.765055i$	$8.825277i$		$\mp 7.12050i$
-0.008131	$\pm 0.014351i$	$\pm 0.014351i$	$0.071755i$	$0.071755i$	-0.000843	$\pm 0.0045i$
			$-0.071755i$	$-0.071755i$		$\mp 0.0124i$
	$\pm 0.014351i$	$\pm 0.014351i$	$0.071755i$	$-0.071755i$	-0.000674	$\pm 0.0100i$
			$-0.071755i$	$0.071755i$		$\pm 0.0134i$
1.008131	$\pm 0.014351i$	$\pm 0.071755i$	$0.014351i$	$0.071755i$	-0.001278	$\pm 0.0001i$
			$-0.014351i$	$-0.071755i$		$\mp 0.0010i$
	$\pm 0.014351i$	$\pm 0.071755i$	$0.014351i$	$-0.071755i$	-0.003346	$\pm 0.0569i$
			$-0.014351i$	$0.071755i$		$\pm 0.0579i$
-122.991869	$\pm 1.765055i$	$\pm 1.765055i$	$8.825277i$	$8.825277i$	303.899917	$\pm 7.5278i$
			$-8.825277i$	$-8.825277i$		$\mp 6.8862i$
	$\pm 1.765055i$	$\pm 1.765055i$	$8.825277i$	$-8.825277i$	-10.195921	$\mp 1.2234i$
			$-8.825277i$	$8.825277i$		$\mp 1.6438i$

Table 3.4: The parameters obtained from $\Gamma_1(5)$. Using (3.19) and $\sum_i m_i = \sqrt{\epsilon_1 \epsilon_2} Q$, we can get the values for α_i 's and Q .

$\zeta = e^{2\pi i \tau}$	m_0	m_1	m_2	m_3	U	a
$\frac{1}{2}$	$\pm \frac{i}{4\pi}$	$\pm \frac{i\sqrt{109}}{2\pi}$	$\frac{2i}{\pi}$	$\frac{27i}{4\pi}$	$\frac{595}{48\pi^2}$	No Pure Imaginary Solution
			$-\frac{2i}{\pi}$	$-\frac{27i}{4\pi}$		
	$\pm \frac{i}{4\pi}$	$\pm \frac{i\sqrt{109}}{2\pi}$	$\frac{2i}{\pi}$	$-\frac{27i}{4\pi}$	$-\frac{269}{48\pi^2}$	
			$-\frac{2i}{\pi}$	$\frac{27i}{4\pi}$		
$\frac{1}{2}$	$\pm \frac{i}{4\pi}$	$\pm \frac{2i}{\pi}$	$\frac{i\sqrt{109}}{2\pi}$	$\frac{27i}{4\pi}$	$\frac{-665+108\sqrt{109}}{48\pi^2}$	No Pure Imaginary Solution
			$-\frac{i\sqrt{109}}{2\pi}$	$-\frac{2i}{\pi}$		
	$\pm \frac{i}{4\pi}$	$\pm \frac{2i}{\pi}$	$\frac{i\sqrt{109}}{2\pi}$	$-\frac{27i}{4\pi}$	$\frac{-665-108\sqrt{109}}{48\pi^2}$	
			$-\frac{i\sqrt{109}}{2\pi}$	$\frac{27i}{4\pi}$		
2	$\pm \frac{i}{2\pi}$	$\pm \frac{i\sqrt{109}}{\pi}$	$\frac{27i}{2\pi}$	$\frac{4i}{\pi}$	$\frac{455}{3\pi^2}$	No Pure Imaginary Solution
			$-\frac{27i}{2\pi}$	$-\frac{4i}{\pi}$		
	$\pm \frac{i}{2\pi}$	$\pm \frac{i\sqrt{109}}{\pi}$	$\frac{27i}{2\pi}$	$-\frac{4i}{\pi}$	$\frac{23}{3\pi^2}$	
			$-\frac{27i}{2\pi}$	$\frac{4i}{\pi}$		

2	$\pm \frac{i}{2\pi}$	$\pm \frac{4i}{\pi}$	$\frac{27i}{2\pi}$	$\frac{i\sqrt{109}}{\pi}$	$\frac{125+54\sqrt{109}}{3\pi^2}$	No Pure Imaginary Solution
			$-\frac{27i}{2\pi}$	$-\frac{i\sqrt{109}}{\pi}$		
	$\pm \frac{i}{2\pi}$	$\pm \frac{4i}{\pi}$	$\frac{27i}{2\pi}$	$-\frac{i\sqrt{109}}{\pi}$	$\frac{125-54\sqrt{109}}{3\pi^2}$	
			$-\frac{27i}{2\pi}$	$\frac{i\sqrt{109}}{\pi}$		
-1	\emptyset	\emptyset	\emptyset	\emptyset	\emptyset	\emptyset

Table 3.5: The parameters obtained from $\Gamma_0(6)$. Using (3.19) and $\sqrt{\epsilon_1\epsilon_2}Q$, we can get the values for α_i 's and Q .

$\zeta = e^{2\pi i\tau}$	m_0	m_1	m_2	m_3	U	a
$\frac{1}{2}$	$\pm \frac{i}{16\pi}$	$\pm \frac{i}{8\pi}$	$\frac{i}{2\pi}$	$\frac{i}{16\pi}$	$\frac{11}{768\pi^2}$	$\mp 0.0126i$
			$-\frac{i}{2\pi}$	$-\frac{i}{16\pi}$		$\mp 0.0130i$
	$\pm \frac{i}{16\pi}$	$\pm \frac{i}{8\pi}$	$\frac{i}{2\pi}$	$-\frac{i}{16\pi}$	$-\frac{7}{256\pi^2}$	$\pm 0.0236i$
			$-\frac{i}{2\pi}$	$\frac{i}{16\pi}$		$\pm 0.0242i$
2	$\pm \frac{i}{8\pi}$	$\pm \frac{i}{4\pi}$	$\frac{i}{8\pi}$	$-\frac{i}{2\pi}$	$\frac{7}{48\pi^2}$	$\mp 0.0619i$
			$-\frac{i}{8\pi}$	$\frac{i}{2\pi}$		$\mp 0.0631i$
	$\pm \frac{i}{8\pi}$	$\pm \frac{i}{4\pi}$	$\frac{i}{8\pi}$	$\frac{i}{2\pi}$	$\frac{7}{48\pi^2}$	$\mp 0.1457i$
			$-\frac{i}{8\pi}$	$-\frac{i}{2\pi}$		$\mp 0.1457i$

Table 3.6: The parameters obtained from $\Gamma_0(8)$. Using (3.19) and $\sqrt{\epsilon_1\epsilon_2}Q$, we can get the values for α_i 's and Q .

$\zeta = e^{2\pi i\tau}$	m_0	m_1	m_2	m_3	U	a
$\frac{1-i\sqrt{3}}{2}$	$\pm \frac{i}{6\sqrt{3}\pi}$	$\pm \frac{i}{6\sqrt{3}\pi}$	$\frac{i}{6\sqrt{3}\pi}$	$\frac{i\sqrt{3}}{2\pi}$	$-\frac{i(33i+25\sqrt{3})}{162\pi^2}$	No Pure Imaginary Solution
			$-\frac{i}{6\sqrt{3}\pi}$	$-\frac{i\sqrt{3}}{2\pi}$		
	$\pm \frac{i}{6\sqrt{3}\pi}$	$\pm \frac{i}{6\sqrt{3}\pi}$	$\frac{i}{6\sqrt{3}\pi}$	$-\frac{i\sqrt{3}}{2\pi}$	$-\frac{i(3i+8\sqrt{3})}{81\pi^2}$	
			$-\frac{i}{6\sqrt{3}\pi}$	$\frac{i\sqrt{3}}{2\pi}$		
$\frac{1+i\sqrt{3}}{2}$	$\pm \frac{i}{6\sqrt{3}\pi}$	$\pm \frac{i}{6\sqrt{3}\pi}$	$\frac{i}{6\sqrt{3}\pi}$	$\frac{i\sqrt{3}}{2\pi}$	$\frac{i(-33i+25\sqrt{3})}{162\pi^2}$	No Pure Imaginary Solution
			$-\frac{i}{6\sqrt{3}\pi}$	$-\frac{i\sqrt{3}}{2\pi}$		
	$\pm \frac{i}{6\sqrt{3}\pi}$	$\pm \frac{i}{6\sqrt{3}\pi}$	$\frac{i}{6\sqrt{3}\pi}$	$-\frac{i\sqrt{3}}{2\pi}$	$\frac{i(-3i+8\sqrt{3})}{81\pi^2}$	
			$-\frac{i}{6\sqrt{3}\pi}$	$\frac{i\sqrt{3}}{2\pi}$		

			$-\frac{i}{6\sqrt{3}\pi}$	$\frac{i\sqrt{3}}{2\pi}$		Solution
--	--	--	---------------------------	--------------------------	--	----------

Table 3.7: The parameters obtained from $\Gamma_0(9)$. Using (3.19) and $\sqrt{\epsilon_1\epsilon_2}Q$, we can get the values for α_i 's and Q .

Based on the above calculations, there are some remarks we can make:

- One may check that the elliptic curves parametrized by these $m_i \in i\mathbb{R}$ and $\zeta, U \in \mathbb{C}$ have the same j -invariants as in Table 3.8 for the six Belyi maps.

$\Gamma(3)$	0
$\Gamma_0(4) \cap \Gamma(2)$	$\frac{35152}{9}$
$\Gamma_1(5)$	$\frac{131072}{9}$
$\Gamma_0(6)$	-3072
$\Gamma_0(8)$	$\frac{21952}{9}$
$\Gamma_0(9)$	0

Table 3.8: The j -invariants that correspond to the six index-12 Belyi maps.

- Recall that under $\phi \rightarrow k\phi$, $a \rightarrow ka$ and $U \rightarrow k^2U$. This is consistent with the fact that $a \sim \sqrt{u} \sim \sqrt{U}$.
- For $\Gamma_0(6)$ and $\Gamma_0(9)$, there are no parametrizations whose CFT can be formulated on the torus. Hence, we simply list all the possible solutions to ζ (and m_i and U if there exists) in Table 3.5 and 3.7.
- For $\Gamma_0(8)$, ζ could also be -1 , but there would be no solution for m_i and U , just like the case for $\zeta = -1$ in $\Gamma_0(6)$.
- It is obvious that for each dessin, the parametrizations for different ζ 's are related by triality¹⁰

$$\zeta \leftrightarrow \zeta' = \frac{1}{\zeta} \leftrightarrow \zeta'' = 1 - \zeta. \quad (3.32)$$

This is explicitly listed in Table 3.9. In particular, the two rows for $\Gamma_1(5)$ are also

¹⁰Since it is not really in the strong or weak coupling regime for some cases, we may refer to this as ‘‘S-like-duality’’.

Dessin	ζ	ζ'	ζ''
$\Gamma(3)$	$\frac{1}{2}(1 \pm i\sqrt{3})$	$\frac{1}{2}(1 \mp i\sqrt{3})$	$\frac{1}{2}(1 \mp i\sqrt{3})$
$\Gamma_0(4) \cap \Gamma(2)$	2	$\frac{1}{2}$	-1
$\Gamma_1(5)$	0.008065	123.991869	0.991935
	-0.008131	-122.991869	1.008131
$\Gamma_0(6)$	2	$\frac{1}{2}$	-1
$\Gamma_0(8)$	2	$\frac{1}{2}$	-1
$\Gamma_0(9)$	$\frac{1}{2}(1 \pm i\sqrt{3})$	$\frac{1}{2}(1 \mp i\sqrt{3})$	$\frac{1}{2}(1 \mp i\sqrt{3})$

Table 3.9: The parametrizations for each case are S-like-duals.

related by triality: $1 - 123.991869 = -122.991869$. Moreover, there are two cases with $|\zeta| = |(1 \pm i\sqrt{3})/2| = 1$, which are exactly the dessins whose Belyi maps have j -invariant 0.

Conformal Blocks Using the data obtained above and the AGT correspondence, we can therefore compute the corresponding CBs. Recall that $\mathcal{B} \equiv \mathcal{B}_\alpha(\alpha_i|\zeta)$ could be computed perturbatively in terms of the instanton numbers. As the analytic result is tedious even for the perturbative expansion, we give the expression to linear order here:

$$\mathcal{B} = 1 + \frac{1}{8\epsilon_1\epsilon_2((\epsilon_1 + \epsilon_2)^2 - 4a^2)} (-4a^2 + 4m_3'^2 - 4m_1'^2 + 4(m_3' + m_1')(\epsilon_1 + \epsilon_2) + (\epsilon_1 + \epsilon_2)^2) \times (-4a^2 + 4m_0'^2 - 4m_2'^2 + 4(m_0' + m_2')(\epsilon_1 + \epsilon_2) + (\epsilon_1 + \epsilon_2)^2) \zeta + \mathcal{O}(\zeta^2). \quad (3.33)$$

For $\Gamma_1(5)$, we have the weak coupling regime with $\zeta = 0.008065, -0.008131$, and therefore we can apply the perturbative expansion for the CB. Moreover, as an example, let us focus on the case with $\epsilon_1 = -\epsilon_2$, i.e., $c = 1$ CBs. This is a nice and interesting case as only $F^{(0,g)}$ would contribute to the holomorphic anomaly equation in Appendix A, and hence recovers the usual genus expansion of topological strings. As discussed in [40], the $F^{(n,g)}$ expansion gives refined information of the cohomology of the moduli space of the BPS states, and in particular, the $\epsilon_1 + \epsilon_2 = 0$ slice gives the complex structure invariant indices. Moreover, there would be no extra shift for the masses when mapping to CFT parameters. In such case, the above expansion for \mathcal{B} reduces to

$$\mathcal{B} = 1 + \frac{1}{32a^2\epsilon_1^2} (-4a^2 + 4m_0'^2 - 4m_2'^2) (-4a^2 + 4m_3'^2 - 4m_1'^2) \zeta + \mathcal{O}(\zeta^2). \quad (3.34)$$

Using the data in Table 3.4, we consider the parametrizations given by $\pm\phi_{\text{SW,basic}}$. When m_i and a are pure imaginary (namely $\phi_{\text{SW,basic}}$ in this case), we simply take

$\epsilon_1 = -\epsilon_2 = i$. When m_i and a are real (namely $-\phi_{\text{SW,basic}}$ in this case), we simply take $\epsilon_1 = -\epsilon_2 = 1$. For instance, with $m_0 = m_3 = 0.01423i$ and $m_1 = m_2 = 0.07116i$, we have $a = 0.0103i$. Therefore,

$$\mathcal{B} = 1 + 0.116284\zeta - 0.0587214\zeta^2 + 0.039343\zeta^3 + 0.0297279\zeta^4 + \mathcal{O}(\zeta^5). \quad (3.35)$$

As $\zeta = 0.008065$, we get $\mathcal{B} = 1.00094$. Likewise, for $\zeta = -0.008131$, if we consider $m_0 = m_1 = 0.014351$, $m_2 = m_3 = -0.071755$ and $a = 0.0124$, we have $\mathcal{B} = 1.00064$. In general, for parametrizations following (3.31), it is straightforward to see that $m_{i,\text{imaginary}}$ and $m_{i,\text{real}}$ would give the same result for \mathcal{B} .

Minimal models When $Q \neq 0$, we have discrete parametrizations originated from the dessins. Therefore, it is natural to conjecture that each parametrization corresponds to the spectrum of certain $c < 1$ minimal models as Q is always pure imaginary. Furthermore, when $Q = 0$ which becomes invariant under the scaling factor k , we have continuous parametrizations for $c = 1$ CBs. In particular, the limit $c \rightarrow 1$ for minimal models gives rise to the Runkel-Watts theory, whose well-definedness was discussed in [41]. Indeed, the spectrum also becomes continuous for minimal models as $c \rightarrow 1$.

4 Conclusions and Outlook

We have seen that each dessin gives specific parametrizations for the gauge theories and hence for the CFTs. However, it is still not known whether/how these values would give any special physical interpretations. It could be possible that these parametrizations have correspondence to the spectra of minimal models.

We could also study the gravity solutions for the corresponding holographic duals of Liouville CFTs. For instance, it is immediate to get the AdS radius and certain information for black holes or thermal gas in AdS from the central charge. Recently, (super) Liouville theory in AdS₂ also entered the study of AdS₂/CFT₁ [42]. Moreover, for 3d dS space, it was also shown in [43] that the spectrum of conical defects has a one-to-one correspondence with the spectrum in Liouville theory. It would be interesting to explore these topics in future.

Acknowledgement

OF wishes to thank R. Santachiara for useful discussions on the topic of this note, as well as related topics. OF is supported by the Australian Research Council. YHH would like to thank STFC for grant ST/J00037X/1. EH would like to thank STFC for the PhD studentship.

A The B-model and Omega Deformations

When mapping gauge theory/SW geometry parameters to CFT parameters, we need to include a factor of $\frac{1}{\sqrt{\epsilon_1 \epsilon_2}}$, which would lead to divergence under the flat space limit $\epsilon_{1,2} \rightarrow 0$. Here, we discuss a way in terms of topological B-model so that the SW geometry is still physically meaningful when $\epsilon_{1,2}$ are non-zero.

Recall that we have related $\mathcal{N} = 2$ gauge theories to A-model topological strings. The mirror in B-model is defined by the equation

$$vw + f(x, y) = 0, \quad (\text{A.1})$$

which is a CY_3 that can be considered as fibration of $uv = \text{const}$ over the Riemann surface $f(x, y)$. In particular, $f(x, y) = 0$ can be identified as the SW curve Σ . Denote the multiplicity of a BPS state in this 5d theory as N^β , where β is essentially the charge of the BPS state¹¹. Mathematically, the BPS configuration can be defined by a (complex) one-dimensional sheaf \mathcal{F} (plus certain section in $H^0(\mathcal{F})$) such that

$$\beta = \text{ch}_2(\mathcal{F}), \quad n = \chi(\mathcal{F}), \quad (\text{A.2})$$

where $\beta \in H_2(\mathcal{M}, \mathbb{Z})$ and $n \in \mathbb{Z}$.

The topological string amplitude then has the expansion

$$F(\epsilon_1, \epsilon_2, t) = \log(Z) = \sum_{n,g=0}^{\infty} (\epsilon_1 + \epsilon_2)^{2n} (\epsilon_1 \epsilon_2)^{g-1} F^{(n,g)}(t), \quad (\text{A.3})$$

where Z is known as the (refined) Pandharipande-Thomas (PT) partition function, and g stands for the genus while t denotes the Kähler parameter measuring the volume of a curve in β , which can be identified as the Coulomb parameter a as we are focusing on $\text{SU}(2)$ gauge group in this paper [39, 40, 44]. In particular, when $n = g = 0$, $F^{(0,0)}$ is the prepotential \mathcal{F} . In the limit $\epsilon_{1,2} \rightarrow 0$, the PT partition function is naturally identified as the Nekrasov partition function at leading order:

$$\log(Z) = (\epsilon_1 \epsilon_2)^{-1} F^{(0,0)}. \quad (\text{A.4})$$

Moreover, $F^{(0,1)}$ and $F^{(1,0)}$ can also be determined using the metric on \mathcal{M} and the discriminant of Σ as in Equation (3.22) and (3.23) in [39]. Then $F^{(n,g)}$ with higher $(g+n)$ can be deduced from the (*generalized*) *holomorphic anomaly equation* [39, 40, 44]

$$\bar{\partial}_{\bar{i}} F^{(n,g)} = \frac{1}{2} \bar{C}_{\bar{i}}^{jk} \left(D_j D_k F^{(n,g-1)} + \sum_{m,h}' D_j F^{(m,h)} D_k F^{(n-m,g-h)} \right), \quad g+n > 1, \quad (\text{A.5})$$

¹¹More precisely, we should also include the indices denoting the $\text{SU}(2)_L \times \text{SU}(2)_R$ spin representations, but for our purpose here, it suffices to label it with the topological data β only. For more details, see for example [44].

where the three-point coupling \bar{C}_i^{jk} is given in [39, 40], and D_i is the covariant derivative. The prime in the sum indicates the omission of $(m, h) = (0, 0), (n, g)$. We also require the first term on the right hand side to vanish if $g = 0$.

Therefore, the non-zero $\epsilon_{1,2}$ would also make sense for the SW theory physically as the prepotential generates the topological string amplitudes. Hence, we could avoid the divergence when mapping the gauge theory parameters to CFT parameters as in §3.

Shift of Parameters Notice that we only have even $2n$ in the string amplitude expansion. However, there could be odd terms in the Nekrasov expansion especially for theories with massive flavours. It was argued in [39] that the odd terms can be eliminated by a shift/redefinition of the mass parameters:

$$m'_i = m_i - \frac{\epsilon_1 + \epsilon_2}{2}, \quad (\text{A.6})$$

where m_i is the mass in the Nekrasov partition function and m'_i is the physical mass in the AGT correspondence¹².

B Brane Configurations

B.1 The Type IIA Brane Configuration

A type IIA configuration of parallel NS/D5-branes joined by D4-branes can be represented in M theory as a single M5-brane with a more complicated world history.

Before we write the rule for finding the Seiberg-Witten curve, we need to find out whether we have a $U(N)$ or an $SU(N)$ gauge theory. This is discussed in [47], and goes as follows.

First, consider D5-branes and D4-branes in type IIA superstring theory. The world-volume of a D5-brane is described as follows. D5-branes are located at $x^7 = x^8 = x^9 = 0$ and, in a semi-classical approximation, at fixed values of x^6 . The world-volume of D5-branes are parameterised by values of x^0, x^1, \dots, x^5 . In addition, D4-branes are parameterised by x^0, x^1, x^2, x^3 and x^6 . D4-branes have their x^6 -coordinate finite so that they terminate on D5-branes. We need to introduce a complex variable $v = x^4 + ix^5$. Classically, every D4-brane is located at a definite value of v . Since a D4-brane ending on a D5-brane creates a *dimple* in the D5-brane, the value x^6 is the value measured at

¹²An alternative holomorphic anomaly equation known as the extended holomorphic anomaly equation was introduced in [45]. It involves the odd terms and reproduces the Nekrasov expansion. However, there could be some issue with holomorphicity and modularity as discussed in [39, 46], so we would still adopt the recipe with only even terms.

$v = \infty$, far from the disturbance created by the D4-brane. By minimizing the volume of the D5-brane, at large v , we obtain

$$x^6 = k \ln|v| + \text{const.} \quad (\text{B.1})$$

This is not well-defined for large v . Nevertheless, with D4-branes attached to the left and to the right of the D5-brane, we have

$$x^6 = k \sum_{i=1}^{q_L} \ln|v - a_i| - k \sum_{j=1}^{q_R} \ln|v - b_j| + \text{const}, \quad (\text{B.2})$$

where a_i and b_j are the v -values, or x^6 -coordinates of D4-branes ending on the left and right respectively. Now x^6 is well-defined for large v if and only if $q_L = q_R$, that is, if the forces on both sides are balanced. For infrared divergence, we need to consider the motion of the D4-branes, whose movement causes the D5-brane to move. The motion of a D5-brane contributes to the kinetic energy of the D4-brane. The D5-brane kinetic energy is given by $\int d^4x d^2v \sum_{\mu=0}^3 \partial_\mu x^6 \partial^\mu x^6$. Therefore, with x^6 in (B.2), we have

$$k^2 \int d^4x d^2v \left| \text{Re} \left(\sum_i \frac{\partial_\mu a_i}{v - a_i} - \sum_j \frac{\partial_\mu b_j}{v - b_j} \right) \right|^2. \quad (\text{B.3})$$

This integral converges if and only if

$$\partial_\mu \left(\sum_i a_i - \sum_j b_j \right) = 0, \quad (\text{B.4})$$

so that

$$\sum_i a_i - \sum_j b_j = q_\alpha, \quad (\text{B.5})$$

where q_α is characteristic of α -th plane. From the D4-brane point of view, (B.5) means the U(1) part of U(k) for k D4-branes between two D5-branes are frozen. This is because $\sum_i a_i$ is the scalar part of U(1) vector multiplet in one factor U(k_α) and $\sum_j b_j$ is the scalar part of the U(1) vector multiplet in the factor U($k_{\alpha+1}$). Since, following (B.5), the difference is fixed by supersymmetry, the entire U(1) vector multiplet is missing, and we have SU(N).

B.2 The M-theory Brane Configuration

The world-volume of the M5-brane is such that,

1. It has arbitrary values in the first \mathbb{M}^4 coordinates x^0, \dots, x^3 , and is located at $x^7 = x^8 = x^9 = 0$;
2. In the remaining four coordinates, which parametrize a 4-manifold $Q \cong \mathbb{R}^3 \times S^1$, D5-brane worldvolume spans a 2d surface Σ ;
3. The $\mathcal{N} = 2$ supersymmetry means we give Q the complex structure in which $v = x^4 + ix^5$ and $s = x^6 + ix^{10}$ are holomorphic, then Σ is a complex Riemann surface in Q . This makes $\mathbb{M}^4 \times \Sigma$ a supersymmetric cycle in the sense of [48] and so it ensures spacetime supersymmetry.

When projected to type IIA brane diagrams, Σ has different components described locally by saying that s is constant (the D5-branes) or that v is constant (the D4-branes). In type IIA, different components can meet and singularity appears in there. However, in going to M theory, singularities disappear. Hence, for generic values of parameters, Σ will be a smooth Riemann surface in Q .

C Congruence Subgroups of the Modular Group

In this appendix, we very briefly recall some essential details regarding the modular group $\Gamma \equiv \Gamma(1) = \text{PSL}(2, \mathbb{Z}) = \text{SL}(2, \mathbb{Z}) / \{\pm I\}$, the group of linear fractional transformations $\mathbb{Z} \ni z \rightarrow \frac{az+b}{cz+d}$, with $a, b, c, d \in \mathbb{Z}$ and $ad - bc = 1$. It is generated by the transformations T and S defined by

$$T(z) = z + 1 \quad , \quad S(z) = -1/z \quad . \quad (\text{C.1})$$

The presentation of Γ is $\langle S, T | S^2 = (ST)^3 = I \rangle$.

The most important subgroups of Γ are the *congruence* subgroups, defined by having the the entries in the generating matrices S and T obeying some modular arithmetic. Of particular note are the following:

- Principal congruence subgroups:

$$\Gamma(m) := \{A \in \text{SL}(2; \mathbb{Z}) ; A_{ij} \equiv \pm I_{ij} \pmod{m}\} / \{\pm I\} ;$$

- Congruence subgroups of level m : subgroups of Γ containing $\Gamma(m)$ but not any $\Gamma(n)$ for $n < m$;
- Unipotent matrices:

$$\Gamma_1(m) := \left\{ A \in \text{SL}(2; \mathbb{Z}) ; A_{ij} \equiv \pm \begin{pmatrix} 1 & b \\ 0 & 1 \end{pmatrix}_{ij} \pmod{m} \right\} / \{\pm I\} ;$$

- Upper triangular matrices:

$$\Gamma_0(m) := \left\{ \begin{pmatrix} a & b \\ c & d \end{pmatrix} \in \Gamma ; c \equiv 0 \pmod{m} \right\} / \{\pm I\}.$$

In [6, 38], attention is drawn to the conjugacy classes of a particular family of subgroups of Γ : the so-called *genus zero, torsion-free* congruence subgroups:

- *Torsion-free* means that the subgroup contains no element of finite order other than the identity.
- To explain *genus zero*, first recall that the modular group acts on the upper half-plane $\mathcal{H} := \{\tau \in \mathbb{C}, \text{Im}(\tau) > 0\}$ by linear fractional transformations $z \rightarrow \frac{az+b}{cz+d}$. Then \mathcal{H} gives rise to a compactification \mathcal{H}^* when adjoining *cusps*, which are points on $\mathbb{R} \sqcup \infty$ fixed under some parabolic element (i.e. an element $A \in \Gamma$ not equal to the identity and for which $\text{Tr}(A) = 2$). The quotient \mathcal{H}^*/Γ is a compact Riemann surface of genus 0, i.e. a sphere. It turns out that with the addition of appropriate cusp points, the extended upper half plane \mathcal{H}^* factored by various congruence subgroups will also be compact Riemann surfaces, possibly of higher genus. Such a Riemann surface, as a complex algebraic variety, is called a *modular curve*. The genus of a subgroup of the modular group is the genus of the modular curve produced in this way.

The conjugacy classes of the genus zero torsion-free congruence subgroups of the modular group are very rare: there are only 33 of them, with index $I \in \{6, 12, 24, 36, 48, 60\}$, as detailed in [38].

D Elliptic Curves and j -Invariants

Given the Weierstrass function \wp

$$\wp(z | \omega_1, \omega_2) = \frac{1}{z^2} + \sum_{n^2+m^2 \neq 0} \left(\frac{1}{(z + m\omega_1 + n\omega_2)^2} - \frac{1}{(m\omega_1 + n\omega_2)^2} \right), \quad (\text{D.1})$$

where ω_1 and ω_2 are complex-valued vectors that span the lattice $\Lambda = \{m\omega_1 + n\omega_2 : m, n \in \mathbb{Z}\}$, and we can write $\wp(z | \omega_1, \omega_2) = \wp(z | \Lambda)$. The embedding of a torus, as an elliptic curve over \mathbb{C} in the complex projective plane, follows from

$$(\wp'(z))^2 = 4(\wp(z))^3 - g_2\wp(z) - g_3, \quad (\text{D.2})$$

where $\wp'(z)$ is the derivative of $\wp(z)$ with respect to z . Naturally defined on a torus \mathbb{C}/Λ , \wp is doubly-periodic with respect to lattice Λ . This torus can be embedded in the complex projective plane by $z \mapsto [1 : \wp(z) : \wp'(z)]$. Close to the origin, $\wp(z)$ can be expanded as

$$\wp(z|\Lambda) = \frac{1}{z^2} + g_2 \frac{z^2}{20} + g_3 \frac{z^4}{28} + \mathcal{O}(z^6), \quad (\text{D.3})$$

where

$$\begin{aligned} g_2 &= 60 \sum_{(m,n) \neq (0,0)} \left(\frac{1}{m\omega_1 + n\omega_2} \right)^4, \\ g_3 &= 140 \sum_{(m,n) \neq (0,0)} \left(\frac{1}{m\omega_1 + n\omega_2} \right)^6. \end{aligned} \quad (\text{D.4})$$

The summed terms in g_2 and g_3 are the first two Eisenstein series respectively. The Eisenstein series G_{2k} with weight $2k$ are modular forms of weight $2k$, that is, they transform as $G_{2k}(\tau) \mapsto (c\tau + d)^{2k} G_{2k}(\tau)$ under $\text{SL}(2, \mathbb{Z})$ with $\tau = \omega_1/\omega_2$ in upper half-plane \mathbb{H} . If two lattices are related by a multiplication by a non-zero complex number c , then the corresponding curves are isomorphic. The j -invariants are defined as

$$j(\tau) = 1728 \frac{g_2^3}{g_2^3 - 27g_3^2}. \quad (\text{D.5})$$

This definition shows that j -invariant is a weight-zero modular form. From the above discussion, we can see that each isomorphism class of elliptic curves over \mathbb{C} has the same j -invariant.

As the SW curves and Strebel differentials we have are of quartic form, $y^2 = az^4 + bz^3 + cz^2 + dz + q^2$, we can make the substitution (for $q \neq 0$)

$$z = \frac{2q(X+c) - d^2/(2q)}{Y}, \quad y = -q + \frac{1}{2q} \frac{2q(X+c) - d^2/(2q)}{Y} \left(\frac{2q(X+c) - d^2/2q}{Y} - d \right) \quad (\text{D.6})$$

so that the elliptic curve can be expressed in the standard Weierstrass form

$$Y^2 + a_1XY + a_3Y = X^3 + a_2X^2 + a_4X + a_6, \quad (\text{D.7})$$

where

$$a_1 = \frac{d}{q}, \quad a_2 = c - \frac{d^2}{4q^2}, \quad a_3 = 2bq, \quad a_4 = -4aq^2, \quad a_6 = ad^2 - 4acq^2. \quad (\text{D.8})$$

Using SAGE [49], we can compute its j -invariant

$$j = - \frac{((a_1^2 + 4a_2)^2 - 24a_1a_3 - 48a_4)^3}{(a_2a_3^2 - a_1a_3a_4 + a_1^2a_6 - a_4^2 + 4a_2a_6)(a_1^2 + 4a_2)^2 + 8(a_1a_3 + 2a_4)^3 - 9(a_1^2 + 4a_2)(a_1a_3 + 2a_4)(a_3^2 + 4a_6) + 27(a_3^2 + 4a_6)^2}. \quad (\text{D.9})$$

If $q = 0$ such as the Strebel differential for $\Gamma(3)$, we can replace z and y with $1/z$ and y/z^2 respectively to obtain a quartic form with a non-vanishing constant term [50].

References

- [1] L. F. Alday, D. Gaiotto, and Y. Tachikawa, “Liouville Correlation Functions from Four-dimensional Gauge Theories,” *Lett. Math. Phys.* **91** (2010) 167–197, [arXiv:0906.3219 \[hep-th\]](#).
- [2] N. Seiberg and E. Witten, “Electric - magnetic duality, monopole condensation, and confinement in N=2 supersymmetric Yang-Mills theory,” *Nucl. Phys. B* **426** (1994) 19–52, [arXiv:hep-th/9407087](#). [Erratum: Nucl.Phys.B 430, 485–486 (1994)].
- [3] N. Seiberg and E. Witten, “Monopoles, duality and chiral symmetry breaking in N=2 supersymmetric QCD,” *Nucl. Phys. B* **431** (1994) 484–550, [arXiv:hep-th/9408099](#).
- [4] N. A. Nekrasov, “Seiberg-Witten prepotential from instanton counting,” *Adv. Theor. Math. Phys.* **7** no. 5, (2003) 831–864, [arXiv:hep-th/0206161](#).
- [5] D. Gaiotto, “N=2 dualities,” *JHEP* **08** (2012) 034, [arXiv:0904.2715 \[hep-th\]](#).
- [6] Y.-H. He and J. McKay, “N=2 Gauge Theories: Congruence Subgroups, Coset Graphs and Modular Surfaces,” *J. Math. Phys.* **54** (2013) 012301, [arXiv:1201.3633 \[hep-th\]](#).
- [7] Y.-H. He, J. McKay, and J. Read, “Modular Subgroups, Dessins d’Enfants and Elliptic K3 Surfaces,” *J. Comput. Math.* **16** (2013) 271–318, [arXiv:1211.1931 \[math.AG\]](#).
- [8] Y.-H. He and J. McKay, “Eta Products, BPS States and K3 Surfaces,” *JHEP* **01** (2014) 113, [arXiv:1308.5233 \[hep-th\]](#).
- [9] Y.-H. He and J. Read, “Dessins d’enfants in $\mathcal{N} = 2$ generalised quiver theories,” *JHEP* **08** (2015) 085, [arXiv:1503.06418 \[hep-th\]](#).
- [10] Y.-H. He and J. McKay, “Sporadic and Exceptional,” [arXiv:1505.06742 \[math.AG\]](#).
- [11] S. K. Ashok, F. Cachazo, and E. Dell’Aquila, “Children’s drawings from Seiberg-Witten curves,” *Commun. Num. Theor. Phys.* **1** (2007) 237–305, [arXiv:hep-th/0611082](#).
- [12] Y.-H. He, E. Hirst, and T. Peterken, “Machine-Learning Dessins d’Enfants: Explorations via Modular and Seiberg-Witten Curves,” [arXiv:2004.05218 \[hep-th\]](#).
- [13] C. Kozcaz, S. Pasquetti, and N. Wyllard, “A & B model approaches to surface operators and Toda theories,” *JHEP* **08** (2010) 042, [arXiv:1004.2025 \[hep-th\]](#).
- [14] T. Eguchi and K. Maruyoshi, “Penner Type Matrix Model and Seiberg-Witten Theory,” *JHEP* **02** (2010) 022, [arXiv:0911.4797 \[hep-th\]](#).
- [15] D. Poland, S. Rychkov, and A. Vichi, “The Conformal Bootstrap: Theory, Numerical Techniques, and Applications,” *Rev. Mod. Phys.* **91** (2019) 015002, [arXiv:1805.04405 \[hep-th\]](#).

- [16] “Infinite conformal symmetry in two-dimensional quantum field theory,” *Nuclear Physics B* **241** no. 2, (1984) 333 – 380.
- [17] N. Nekrasov and A. Okounkov, *Seiberg-Witten theory and random partitions*, vol. 244, pp. 525–596. 2006. [arXiv:hep-th/0306238](#).
- [18] A. M. Polyakov, “Quantum Geometry of Bosonic Strings,” *Phys. Lett. B* **103** (1981) 207–210.
- [19] D. Harlow, J. Maltz, and E. Witten, “Analytic Continuation of Liouville Theory,” *JHEP* **12** (2011) 071, [arXiv:1108.4417 \[hep-th\]](#).
- [20] J. Teschner, “Liouville theory revisited,” *Class. Quant. Grav.* **18** (2001) R153–R222, [arXiv:hep-th/0104158](#).
- [21] R. J. Rodger, “A pedagogical introduction to the agt conjecture,” Master’s thesis, 2013.
- [22] I. Antoniadis, E. Gava, K. Narain, and T. Taylor, “Topological amplitudes in string theory,” *Nucl. Phys. B* **413** (1994) 162–184, [arXiv:hep-th/9307158](#).
- [23] M. Bershadsky, S. Cecotti, H. Ooguri, and C. Vafa, “Kodaira-Spencer theory of gravity and exact results for quantum string amplitudes,” *Commun. Math. Phys.* **165** (1994) 311–428, [arXiv:hep-th/9309140](#).
- [24] M. Aganagic, A. Klemm, M. Marino, and C. Vafa, “The Topological vertex,” *Commun. Math. Phys.* **254** (2005) 425–478, [arXiv:hep-th/0305132](#).
- [25] A. Iqbal, C. Kozcaz, and C. Vafa, “The Refined topological vertex,” *JHEP* **10** (2009) 069, [arXiv:hep-th/0701156](#).
- [26] L. Bao, V. Mitev, E. Pomoni, M. Taki, and F. Yagi, “Non-Lagrangian Theories from Brane Junctions,” *JHEP* **01** (2014) 175, [arXiv:1310.3841 \[hep-th\]](#).
- [27] M. Taki, “Refined Topological Vertex and Instanton Counting,” *JHEP* **03** (2008) 048, [arXiv:0710.1776 \[hep-th\]](#).
- [28] O. Foda and J.-F. Wu, “From topological strings to minimal models,” *JHEP* **07** (2015) 136, [arXiv:1504.01925 \[hep-th\]](#).
- [29] O. Foda and J.-F. Wu, “A Macdonald refined topological vertex,” *J. Phys. A* **50** no. 29, (2017) 294003, [arXiv:1701.08541 \[hep-th\]](#).
- [30] Y. Tachikawa, *$N=2$ supersymmetric dynamics for pedestrians*, vol. 890. 2014. [arXiv:1312.2684 \[hep-th\]](#).
- [31] N. C. Leung and C. Vafa, “Branes and toric geometry,” *Adv. Theor. Math. Phys.* **2** (1998) 91–118, [arXiv:hep-th/9711013](#).
- [32] A. Gorsky, S. Gukov, and A. Mironov, “SUSY field theories, integrable systems and their stringy / brane origin. 2.,” *Nucl. Phys. B* **518** (1998) 689–713, [arXiv:hep-th/9710239](#).

- [33] S.-S. Kim and F. Yagi, “5d E_n Seiberg-Witten curve via toric-like diagram,” *JHEP* **06** (2015) 082, [arXiv:1411.7903 \[hep-th\]](#).
- [34] E. Girondo and G. González-Diez, *Introduction to Compact Riemann Surfaces and Dessins d’Enfants*. London Mathematical Society Student Texts. Cambridge University Press, 2011.
- [35] G. Jones and D. Singerman, “Belyi Functions, Hypermaps and Galois Groups,” *Bulletin of the London Mathematical Society* **28** no. 6, (11, 1996) 561–590.
- [36] A. Grothendieck, *Esquisse d’un Programme*. 1984.
- [37] M. Mulase and M. Penkava, “Ribbon graphs, quadratic differentials on riemann surfaces, and algebraic curves defined over \bar{q} ,” *Asian J. Math.* **2** (11, 1998) .
- [38] J. McKay and A. Sebbar, “J-invariants of arithmetic semistable elliptic surfaces and graphs,” *CRM Proceedings and Lecture Notes* (2001) 119–130.
- [39] M.-x. Huang, A.-K. Kashani-Poor, and A. Klemm, “The Ω deformed B-model for rigid $\mathcal{N} = 2$ theories,” *Annales Henri Poincare* **14** (2013) 425–497, [arXiv:1109.5728 \[hep-th\]](#).
- [40] M.-x. Huang and A. Klemm, “Direct integration for general Ω backgrounds,” *Adv. Theor. Math. Phys.* **16** no. 3, (2012) 805–849, [arXiv:1009.1126 \[hep-th\]](#).
- [41] I. Runkel and G. Watts, “A Nonrational CFT with $c = 1$ as a limit of minimal models,” *JHEP* **09** (2001) 006, [arXiv:hep-th/0107118](#).
- [42] M. Beccaria, H. Jiang, and A. A. Tseytlin, “Supersymmetric Liouville theory in AdS₂ and AdS/CFT,” *JHEP* **11** (2019) 051, [arXiv:1909.10255 \[hep-th\]](#).
- [43] D. Klemm and L. Vanzo, “De Sitter gravity and Liouville theory,” *JHEP* **04** (2002) 030, [arXiv:hep-th/0203268](#).
- [44] M.-X. Huang, A. Klemm, and M. Poretschkin, “Refined stable pair invariants for E-, M- and $[p, q]$ -strings,” *JHEP* **11** (2013) 112, [arXiv:1308.0619 \[hep-th\]](#).
- [45] D. Krefl and J. Walcher, “Extended Holomorphic Anomaly in Gauge Theory,” *Lett. Math. Phys.* **95** (2011) 67–88, [arXiv:1007.0263 \[hep-th\]](#).
- [46] M. Aganagic, V. Bouchard, and A. Klemm, “Topological Strings and (Almost) Modular Forms,” *Commun. Math. Phys.* **277** (2008) 771–819, [arXiv:hep-th/0607100](#).
- [47] E. Witten, “Solutions of four-dimensional field theories via M theory,” *Nucl. Phys. B* **500** (1997) 3–42, [arXiv:hep-th/9703166](#).
- [48] K. Becker, M. Becker, and A. Strominger, “Five-branes, membranes and nonperturbative string theory,” *Nucl. Phys. B* **456** (1995) 130–152, [arXiv:hep-th/9507158](#).

- [49] The Sage Developers, *SageMath, the Sage Mathematics Software System (Version 9.1)*, 2020. <https://www.sagemath.org>.
- [50] I. Connell, “Elliptic Curve Handbook,”
<https://webs.ucm.es/BUCM/mat/doc8354.pdf>.